

Randomization Tests for Monotone Spillover Effects

Shunzhuang Huang* Xinran Li† Panos Toulis‡

January 5, 2025

Abstract

Randomization tests have gained popularity for causal inference under network interference because they are finite-sample valid with minimal assumptions. However, existing procedures are limited as they primarily focus on the existence of spillovers through sharp null hypotheses on potential outcomes. In this paper, we expand the scope of randomization procedures in network settings by developing new tests for the monotonicity of spillover effects. These tests offer insights into whether spillover effects increase, decrease, or exhibit “diminishing returns” along certain network dimensions of interest. Our approach partitions the network into multiple (possibly overlapping) parts and testing a monotone contrast hypothesis in each sub-network. The test decisions can then be aggregated in various ways depending on how each test is constructed. We demonstrate our method through a re-analysis of a large-scale policing experiment in Colombia, which reveals evidence of monotonicity related to the “crime displacement hypothesis”. In particular, our analysis suggests that crime spillovers on a control street are increasing in the number of nearby streets treated with more intense policing, but the effect is diminishing at higher levels of exposure.

*University of Chicago, Booth School of Business. shunzhuang.huang@chicagobooth.edu

†University of Chicago, Department of Statistics. xinranli@uchicago.edu

‡University of Chicago, Booth School of Business. panos.toulis@chicagobooth.edu

PT acknowledges support from NSF SES-2419009. All authors wish to thank Azeem Shaikh and Chris Hansen for valuable feedback and comments.

1 Introduction

In many real-world experimental settings, the treatment effect on some units may depend on the treatments administered to other units through a network. The presence of such spillover effects violates the classical “no interference” assumption (Cox, 1958; Rubin, 1980) and presents unique methodological challenges in the estimation of treatment effects.

To address this problem, a recent line of research in causal inference under interference has leveraged the classical Fisherian randomization test (Fisher, 1935). The key idea is to condition on a subset of units and treatment assignments for which potential outcomes are imputable under the null hypothesis of no spillover effect (Athey et al., 2018; Basse et al., 2019; Puelz et al., 2022), and perform a *conditional* randomization test. The resulting procedures are valid in finite samples without requiring a correct specification of the outcome model and are generally straightforward to implement in practice.

However, the scope of these procedures is currently limited to testing the sharp equality of potential outcomes under certain levels of treatment exposure; e.g., testing whether a unit’s outcomes are unaffected by having zero or at least one treated neighbor, holding the unit’s individual treatment fixed. While such sharp tests can be useful to understand the existence and overall magnitude of spillover effects, they cannot be used to determine how the spillover effect varies as a function of treatment exposure.

In this paper, we expand the scope of existing randomization procedures to null hypotheses related to the monotonicity of spillover effects. We allow treatment exposure to take values in a totally ordered set —e.g., 0, 1, 2, or more treated neighbors— and test whether higher treatment exposure leads to better or worse outcomes. The key idea underlying our test is to split the network into multiple, possibly overlapping, sub-networks, and use each sub-network to test a single monotone hypothesis on treatment exposure. We then combine the separate test results while controlling for possible dependence between these tests. The final procedure is finite-sample valid and is straightforward to implement, especially under Bernoulli randomized designs.

We apply our procedure to re-examine a large-scale policing experiment in Medellín, Colombia conducted by [Collazos et al. \(2021\)](#). The goal of our analysis is to test whether crime spillovers on a control street are monotone with respect to the number of neighboring treated streets. Our results provide insights related to the “crime displacement hypothesis” and may be relevant for crime prevention policies. Specifically, we find that a control street is negatively affected from being exposed to nearby streets that are treated with more intense policing, in a way that is monotone in the total number of treated neighboring streets. In addition, we find evidence of “diminishing returns”, where the magnitude of the crime spillover effect diminishes at higher levels of exposure to treated neighboring streets.

Our proposed methodology builds upon existing methodologies in the randomization inference literature. First, we leverage existing methodologies from conditional randomization tests under network interference ([Athey et al., 2018](#); [Basse et al., 2019](#); [Puelz et al., 2022](#); [Basse et al., 2024](#)). While these procedures are finite-sample valid for testing certain types of causal effects under network interference, they are not applicable for monotone null hypotheses. To address this limitation, we leverage recent results in testing bounded null hypotheses under no interference ([Caughey et al., 2023](#)), and extend the related methodology to settings with interference. Furthermore, our network-splitting strategy outlined above utilizes the idea of approximate evidence factors developed by [Rosenbaum \(2011\)](#). Notably, [Zhang and Zhao \(2024\)](#) also utilized this idea to construct conditional randomization tests in a recursive manner. This recursive construction, however, is largely context-specific and it is not directly applicable to our monotone hypothesis.

The rest of the paper is organized as follows. Section 2 introduces the general setup, and provides the formal definition of our monotone hypothesis. We then outline the proposed method in Section 3. In Section 4, we present a detailed description of our method tailored to non-uniform Bernoulli designs. More general experimental designs are considered in Section 5. In Section 6, we show the validity and power of our tests through simulated studies. In Section 7, we apply our methodology to the Medellín data. Section 8 concludes the paper.

2 Problem Setup

Consider a finite population of N units indexed by $i \in [N] := \{1, 2, \dots, N\}$. The treatment for unit i is denoted as $Z_i \in \{0, 1\}$. The population treatment is the column vector $Z := (Z_1, Z_2, \dots, Z_N) \in \{0, 1\}^N$, and follows a known treatment assignment design $Z \sim P(Z)$. Vector Z_S will denote the sub-vector of Z that corresponds to the units in S . The potential outcome for unit i under population treatment $z \in \{0, 1\}^N$ is denoted as $Y_i(z) \in \mathbb{R}$, and $Y(z) := (Y_1(z), Y_2(z), \dots, Y_N(z))$ is the potential outcome (column) vector for the whole population. These potential outcomes are fixed under the randomization framework. Let $Z^{\text{obs}} \sim P(Z^{\text{obs}})$ be the observed treatments and $Y^{\text{obs}} = Y(Z^{\text{obs}})$ be the observed outcomes. Each unit i may also have covariates $X_i \in \mathbb{R}^p$, which could include pre-treatment outcomes.

Under the classical “stable unit treatment value assumption” (Rubin, 1980), a unit’s potential outcome depends solely on its treatment Z_i , so that $Y_i(Z) = Y_i(Z')$ for any unit i and any assignments Z, Z' for which $Z_i = Z'_i$. Under interference, this assumption is no longer plausible. However, without any restrictions on interference, each unit may have 2^N different potential outcomes, which is computationally prohibitive. To make progress, we follow a common approach and assume a low-dimensional summary of interference (Hong and Raudenbush, 2006), also known as “treatment exposure” (Aronow and Samii, 2017) or “effective treatment” (Manski, 2013).

Assumption 1 (Treatment Exposure). *There exists a finite set \mathcal{W} endowed with an equality and ordering relation, exposure mapping functions $w_i : \{0, 1\}^N \rightarrow \mathcal{W}$, $i \in [N]$, and potential outcome functions $y_i : \{0, 1\} \times \mathcal{W} \rightarrow \mathbb{R}$, such that*

$$Y_i(z) = y_i(z_i, w_i(z)) \text{ for all } i, z. \tag{1}$$

In many settings, the exposure function for some unit i may depend only on treatments of a subset of units $S \subseteq [N]$, i.e., $w_i(z) = w_i(z')$ for any z, z' for which $z_S = z'_S$. In such settings, we will overload the notation and write $w_i(z_S)$ in place of $w_i(z)$. Set S may vary across i .

Here, $w_i(z)$ is the treatment exposure of unit i under population treatment $z \in \{0, 1\}^N$ due to interference. We note that the above definition of exposure mappings is not unique. For example, any monotone transformation of w_i , or any set \mathcal{W}' defined more “finely” than \mathcal{W} would also satisfy Assumption 1. In this paper, we will focus on a special type of treatment exposure arising from interference due to a network between units, which we introduce below.

Let $\mathcal{G} = (V, E)$ be a network with vertex set $V = [N]$, edge set E , and adjacency matrix $A \in \{0, 1\}^{N \times N}$, representing connections between units (e.g., friendship or geographical proximity). $A_{ij} = 1$ if units i and j share a connection, and we assume this matrix to be symmetric with no self-loops. For each $i \in V$ define the set of neighboring nodes as $\mathcal{N}_i := \{j \in V : (i, j) \in E\}$, and $\mathcal{N}(S) := \bigcup_{i \in S} \mathcal{N}_i$ for any $S \subseteq V$.

Although our methodology is not tied to a particular exposure definition, we will mainly work with the following exposure function throughout the paper unless stated otherwise.

$$w_i(z) = \sum_{j \in [N]} A_{ij} z_j = \sum_{j \in \mathcal{N}_i} z_j = w_i(z_{\mathcal{N}_i}). \quad (2)$$

The definition in Equation (2) implies that the potential outcomes of a unit are affected by the number of direct neighbors of i that are treated under z . In this case, $\mathcal{W} = \{0, 1, \dots, d_{\max}\}$ is the set of all possible exposures, where d_{\max} is the maximum degree of \mathcal{G} . A natural ordering for this set is the partial order on integers.

An important departure of our work from prior literature relates to the ordering of treatment exposures in \mathcal{W} . In previous work on exact randomization tests under network interference, treatment exposure on a unit i is defined as whether any immediate neighbors of i are treated (Basse et al., 2019; Puelz et al., 2022), or as the treatment sub-vector corresponding to all units within a certain distance from i (Athey et al., 2018). In such cases, different values of treatment exposure just correspond to different levels of interference without a particular ordering. In our work, treatment exposures have a natural ordering, and the goal is to test whether such ordering in exposures induces an ordering also on the potential outcomes. We turn to this question next.

2.1 Null hypothesis of monotone spillover effects

Suppose that we have an ordered exposure set (e.g., “number of treated neighbors”) $\mathcal{W} = \{w_1, w_2, \dots, w_K\}$ such that $w_j \leq w_k \Leftrightarrow j \leq k$, where equality is attained if and only if $j = k$.

The central goal of our paper is to test the following *monotone decreasing null hypothesis*:

$$H_0 : y_i(0, w_1) \geq y_i(0, w_2) \geq \dots \geq y_i(0, w_K), \quad \forall i \in [N]. \quad (3)$$

Equivalently, we are testing $K - 1$ hypotheses of the form

$$H_{0k} : y_i(0, w_k) \geq y_i(0, w_{k+1}), \quad \forall i \in [N], \quad (4)$$

for $k \in [K - 1]$, such that $H_0 = \bigcap_{k \in [K-1]} H_{0k}$ can be defined as an intersection hypothesis. Note that the monotone increasing null hypothesis, $y_i(0, w_1) \leq y_i(0, w_2) \leq \dots \leq y_i(0, w_K)$, can also be tested by either flipping the exposure labels or flipping the sign of the outcomes.

Under the network interference with the exposure model in (2), H_0 means that as more of i ’s neighbors are treated, the outcome of i changes in a monotone decreasing manner, even when i ’s own treatment stays fixed. There are several real-world settings where such a question is of scientific interest. We describe some illustrative examples below.

Example 1 (Crime spillovers). The “crime displacement hypothesis” posits that crime prevention efforts in one area may shift criminal activities to other areas in situations where offenders can be mobile. Recent studies, however, also suggest an opposite effect where the benefits of crime prevention extend to nearby areas that were not directly targeted by the intervention (Guerette and Bowers, 2017). In this context, understanding whether spillover effects are affected monotonically by the strength of crime prevention efforts in nearby areas, and whether these effects saturate at certain levels of exposure, is of significant practical interest. While numerous studies examine the existence of crime spillover effects¹, to our best knowledge none have studied the monotonicity of these effects.

¹See, for example, Blattman et al. (2021); Collazos et al. (2021) and Guerette and Bowers (2017) for a review.

Example 2 (Social networks). During Covid-19, [Breza et al. \(2021\)](#) conducted a cluster saturation randomized design to study the effect of stay-at-home messages through social media on peoples’ mobility. The researchers observed a greater reduction in Covid-19 cases in control areas in clusters treated with high-intensity messaging compared to control areas within clusters treated with low-intensity messaging. In our setup, we can frame this question as a monotone spillover hypothesis of Equation (4), where Y measures Covid-19 cases and the exposure is treatment intensity within the unit’s cluster.

Despite its significance, H_0 is challenging to test in finite samples via randomization tests. One key problem is that H_0 is a “non-sharp hypothesis”, which does not allow the imputation of all missing potential outcomes. While recent randomization-based methods have dealt with certain classes of non-sharp hypotheses ([Athey et al., 2018](#); [Basse et al., 2019](#); [Puelz et al., 2022](#)), these methods rely on being able to reduce a non-sharp hypothesis into a sharp hypothesis by appropriately conditioning the test on a subset of the data. Such reduction is not possible in our setting because the ordering relation in Equation (3) cannot, in general, “pin down” the missing potential outcomes, except perhaps for certain limited cases, e.g. when outcomes are binary.

As we will see in the next section, our proposed method addresses this challenge by combining two distinct approaches in constructing randomization tests for non-sharp null hypotheses: one approach tests a “sharper” version of H_{0k} with a conditional Fisherian randomization test, and another approach extends the conditional test on the sharp null towards testing the corresponding non-sharp null of Equation (4). Below, we discuss our method on a high level, leaving details for Sections 4 and 5.

3 Overview of Main Method

In this section, we provide an overview of our proposed method. Conceptually, our method can be described in four key steps:

GENERAL PROCEDURE FOR TESTING THE MONOTONE NULL

- Step 1.** Split the network into $K - 1$ parts in order to test H_{0k} separately within each part.
- Step 2.** Based on the original hypothesis H_{0k} in Equation (4), define a sharper null hypothesis, \tilde{H}_{0k} , that can be tested with existing conditional randomization tests (Athey et al., 2018; Puelz et al., 2022).
- Step 3.** Adapt the test for \tilde{H}_{0k} towards testing H_{0k} by applying the bounded null techniques of Caughey et al. (2023). This requires the use of test statistics with a suitable property of *exposure monotonicity*, which we make concrete below.
- Step 4.** Combine the $K - 1$ individual p -values obtained from each network part towards testing the main hypothesis, H_0 . To this end, we leverage the concept of *stochastically larger than uniform* p -values of Rosenbaum (2011).

Below, we review some important aspects of this procedure, leaving technical details for the sections that follow.

Step 1: Splitting the network. The first step is to split the network, $\mathcal{G} = (V, E)$, into several —possibly overlapping in nodes— sub-networks denoted by $(\mathcal{G}_k)_{k \in [K]}$ where $\mathcal{G}_k = (V_k, E_k)$. The idea is to test H_{0k} within each sub-network \mathcal{G}_k through a conditional randomization test, each producing a finite-sample valid p -value. The test for the monotone null defined in Equation (3) then comes from the combination of these p -values, and the way \mathcal{G} is split is designed to facilitate this combination. We discuss more technical details about such splitting later in Sections 4 and 5.

Step 2: Single contrast hypothesis. The second step is to focus on a sharper version of H_{0k} , defined as follows:

$$\tilde{H}_{0k} : y_i(0, \mathbf{w}_k) = y_i(0, \mathbf{w}_{k+1}), \quad \forall i \in [N]. \tag{5}$$

The null hypothesis in Equation (5) remains a non-sharp null hypothesis as it only compares two out of the $2K$ potential outcomes. However, \tilde{H}_{0k} can be tested using existing methods

from the conditional randomization testing literature (Athey et al., 2018; Basse et al., 2019; Puelz et al., 2022). As we review later, the key idea in these methods is to subset the data in a particular way such that a conditional randomization test is possible within only those control units exposed to either w_k or w_{k+1} .

Step 3: Exposure-monotone test statistics. The next step is to adapt the tests derived for \tilde{H}_{0k} towards testing H_{0k} . This is possible as long as the test statistics in each individual randomization test satisfy the following *exposure-monotone* property.

Definition 1 (Exposure monotonicity). Let $\mathcal{U} \subseteq [N]$ be a subset of units and $\mathcal{Z} \subseteq \{0, 1\}^N$ be a subset of treatments, and write $\mathcal{C} = (\mathcal{U}, \mathcal{Z})$. A test statistic, $t(z, y; \mathcal{C}) : \{0, 1\}^N \times \mathbb{R}^N \rightarrow \mathbb{R}$, is exposure-monotone with respect to \mathcal{C} in the order (w, w') with $w \leq w'$ if (a) its value depends only on the sub-vector of y restricted on units in \mathcal{U} and the sub-vector of z restricted on units in $\mathcal{U} \cup \mathcal{N}(\mathcal{U})$; and (b) for all $z \in \mathcal{Z}$ and $y, \eta, \xi \in \mathbb{R}^N$ with $\eta_i \geq 0 \geq \xi_i \forall i \in \mathcal{U}$,

$$t(z, y_{\eta\xi}; \mathcal{C}) \geq t(z, y; \mathcal{C}), \tag{6}$$

where $y_{\eta\xi,i} = y_i + \mathbb{1}\{w_i(z) = w'\}\eta_i + \mathbb{1}\{w_i(z) = w\}\xi_i$. We will sometimes write the test statistic as $t(z, y; \mathcal{U})$ when \mathcal{Z} is clear from the context.

Intuitively, an exposure-monotone test statistic operates only on a subset of units and treatment assignments, which, as explained later, are selected such that under these treatment assignments, missing potential outcomes can be imputed or bounded by the observed outcomes for the subset of units, usually termed “focal units” (Athey et al., 2018). Moreover, an exposure-monotone statistic is “aligned” with the ordering of outcomes in the null hypothesis: its value increases towards the direction of higher exposure levels and decreases towards the direction of lower exposure levels. This definition extends the concept of “effect increasing test statistics” developed by Caughey et al. (2023) to settings with interference.

One example of an exposure-monotone test statistic is the simple difference-in-means test statistic in two exposure groups. Let $I_i(z, w) = \mathbb{1}\{w_i(z) = w\}$ indicate whether unit i is

exposed to level w under population treatment z . For any $w \leq w'$, define

$$t_{w,w'}^{\text{DiM}}(z, y; \mathcal{U}) = \frac{1}{\sum_{i \in \mathcal{U}} I_i(z, w')} \sum_{i \in \mathcal{U}} I_i(z, w') \psi_1(y_i) - \frac{1}{\sum_{i \in \mathcal{U}} I_i(z, w)} \sum_{i \in \mathcal{U}} I_i(z, w) \psi_0(y_i), \quad (7)$$

where ψ_1 and ψ_0 are non-decreasing functions from \mathbb{R} to \mathbb{R} . This test statistic is the difference in (transformed) sample mean outcomes between units exposed to w' and w , using data only from units in \mathcal{U} . It further allows weighting outcomes by probabilities, such as the conditional probability of unit i being exposed to w' or w , which is easily calculated in certain designs.

Another example is the rank-based statistic of the form

$$t_{w,w'}^{\text{rank}}(z, y; \mathcal{C}) = \sum_{i \in \mathcal{U}} I_i(z, w') \varphi(r_i(y_{\mathcal{U}})), \quad (8)$$

where φ is a non-decreasing function and $r_i(y_{\mathcal{U}})$ is the rank of y_i within $y_{\mathcal{U}} = (y_i : i \in \mathcal{U})$, the outcome sub-vector for units in \mathcal{U} . In case of tied ranks, we define $\varphi(\cdot)$ as the average value of $\varphi(\cdot)$ evaluated at those ranks with ties broken by unit ordering.² We verify the exposure monotonicity of these two statistics in Appendix A.1.

Step 4: Combination of p -values. In the last step, we combine the individual p -values obtained by testing H_{0k} on each sub-network. As a result of network splitting, however, these p -values may be mutually dependent, and so to combine them appropriately we use the concept of *stochastically larger than uniform p -values* defined as follows.

Definition 2 (Stochastically larger than uniform (Brannath et al., 2002; Rosenbaum, 2011)).

A K -dimensional random vector (P_1, \dots, P_K) with support in the K -dimensional unit cube is stochastically larger than uniform if for all $(p_1, \dots, p_K) \in [0, 1]^K$,

$$\mathbb{P}(P_1 \leq p_1, \dots, P_K \leq p_K) \leq p_1 \times \dots \times p_K.$$

Independent p -values are trivially stochastically larger than uniform, but the above definition allows for possibly dependent p -values. A key technical challenge in our method is to

²That is, $r_i > r_j$ if and only if $(y_i > y_j) \vee (y_i = y_j, i > j)$.

split the network in a way such that the resulting p -values will be stochastically larger than uniform. On a high level, our strategy will be to, first, split the node set V into possibly overlapping sets V_1, \dots, V_K . Then, for all $k = 1, \dots, K - 1$, we sequentially compute the p -value for H_{0k} using information only from units in $V_1 \cup V_2 \dots \cup V_k$, as explained in Sections 4 and 5. Such sequential construction leads to stochastically larger than uniform p -values by the following lemma.

Lemma 1 (Rosenbaum (2011), Lemma 3). *If, for all k , P_k is a function of (Q_1, \dots, Q_k) and $\mathbb{P}(P_k \leq p_k | Q_1, \dots, Q_{k-1}) \leq p_k$ for all $p_k \in [0, 1]$ and for all (Q_1, \dots, Q_{k-1}) , then (P_1, \dots, P_K) is stochastically larger than uniform.*

We can combine stochastically larger than uniform p -values into a single valid p -value in certain ways as if they were independent. For example, Fisher’s combination rule,

$$p_{\text{FCT}} := 1 - F_{\chi^2_{2(K-1)}} \left(-2 \sum_{k=1}^{K-1} \log p_k \right), \quad (9)$$

leads to a valid combined p -value p_{FCT} , where $F_{\chi^2_{2(K-1)}}(\cdot)$ is the cumulative distribution function of a $\chi^2_{2(K-1)}$ distribution. That is, if $(p_k)_k$ are stochastically larger than uniform, then $\mathbb{P}(p_{\text{FCT}} \leq \alpha) \leq \alpha$ for all $\alpha \in [0, 1]$. There are other ways apart from Fisher’s rule to aggregate these p -values, such as Stouffer’s and Cauchy’s combination rules as well as Bonferroni’s method, where the Bonferroni’s method is valid even without splitting the network to have stochastically larger than uniform p -values. We discuss other combination methods in Appendix B and advocate for the use of Fisher’s rule in our problem.

4 Methodology under Non-Uniform Bernoulli Design

In this section, we present our main method in settings where the design follows a non-uniform Bernoulli distribution, defined as follows.

Definition 3 (Non-uniform Bernoulli Design). The assignment mechanism $P(Z)$ satisfies

$P(Z = z) = \prod_{i \in [N]} p_i^{z_i} (1 - p_i)^{1 - z_i}$, for $z \in \{0, 1\}^N$, where $p_i \in [0, 1]$ are known treatment probabilities.

The unit treatment probabilities in a non-uniform Bernoulli design can be arbitrary as long as they are known and fixed. For example, p_i could depend on unit covariates, past outcomes, network, or other pre-treatment features of the unit and other units. The primary restriction is that units are treated independently. Obviously, the non-uniform Bernoulli design includes the usual Bernoulli design as a special case, under which the treatment probabilities are identical for all units.

Under the non-uniform Bernoulli design, we first introduce an algorithm to test a single contrast hypothesis H_{0k} in Equation (4), as explained in Steps 2-3 of the general procedure of the previous section. Before presenting our test for H_{0k} , we define certain graph-theoretic concepts that will clarify how we utilize the structure of non-uniform Bernoulli designs to build our randomization test, and how we can extend it towards more flexible designs.

4.1 Preliminary concepts: Module and Module sets

We begin with the concepts of *module* and *module set*, which are crucial in the construction of our tests.

Definition 4. A *module* is a subset of units $\mathcal{S} \subseteq [N]$ that can be partitioned into two disjoint subsets, namely $\mathcal{S} = \mathbf{E}_{\text{foc}}(\mathcal{S}) \cup \mathbf{E}_{\text{rand}}(\mathcal{S})$, such that any pair of units $i, j \in \mathbf{E}_{\text{foc}}(\mathcal{S})$ is disconnected ($A_{ij} = 0$), and their neighborhoods are contained in $\mathbf{E}_{\text{rand}}(\mathcal{S})$; i.e., $\mathcal{N}(\mathbf{E}_{\text{foc}}(\mathcal{S})) \subseteq \mathbf{E}_{\text{rand}}(\mathcal{S})$. We will refer to $\mathbf{E}_{\text{foc}}(\mathcal{S})$ as the set of *eligible focal units* of module \mathcal{S} , and $\mathbf{E}_{\text{rand}}(\mathcal{S})$ as the set of *eligible randomization units* of the module. A *module set* \mathbb{S} is a collection of modules $\{\mathcal{S}_1, \dots, \mathcal{S}_L\}$ such that the eligible randomization units across modules do not overlap; that is, for all $\ell \neq \ell'$, $\mathbf{E}_{\text{rand}}(\mathcal{S}_\ell) \cap \mathbf{E}_{\text{rand}}(\mathcal{S}_{\ell'}) = \emptyset$ holds.

These definitions are illustrated in Figure 1. In the figure, all eligible focal units in a module share the same neighbors and thus receive the same exposure under any treatment

assignment. We call such a module a *uniform* module. Formally, a module \mathcal{S} is uniform if $\mathcal{N}_i = \mathbf{E}_{\text{rand}}(\mathcal{S})$ for all $i \in \mathbf{E}_{\text{foc}}(\mathcal{S})$.

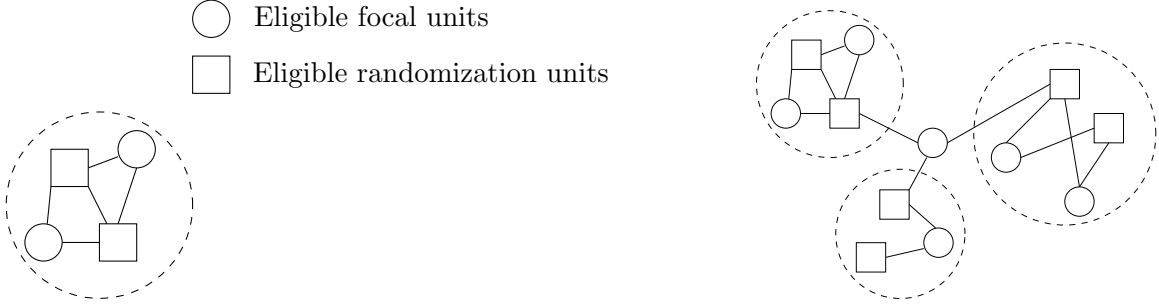


Figure 1: *Left panel:* A uniform module \mathcal{S} . Circles represent eligible focal units and squares represent eligible randomization units. *Right panel:* A module set \mathbb{S} consisting of three uniform modules outlined by dashed circles.

Constructing a module set is computationally straightforward. One approach is to start by randomly sampling a unit j_1 in V , define $\mathcal{S}_1 = \{j_1\} \cup \mathcal{N}_{j_1}$, and then calculate the remainder $V^{(1)} \leftarrow V \setminus \{\mathcal{S}_1 \cup \mathcal{N}(\mathcal{S}_1)\}$. Then, sample another unit j_2 in $V^{(1)}$, define $\mathcal{S}_2 = \{j_2\} \cup \mathcal{N}_{j_2}$, calculate the remainder $V^{(2)} \leftarrow V^{(1)} \setminus \{\mathcal{S}_2 \cup \mathcal{N}(\mathcal{S}_2)\}$, and so on. The process terminates when $V^{(L+1)}$ is empty. As a last step, we may augment each singleton $\mathbf{E}_{\text{foc}}(\mathcal{S}_\ell) = \{j_\ell\}$ with units not in any modules and have exactly the same neighbors as j_ℓ , for each $\ell = 1, \dots, L$. The resulting modules are uniform modules as well. In some applications where far more units always remain in control compared to those that could be treated, $\mathbf{E}_{\text{rand}}(\mathcal{S})$ can be defined to include only the units that could be treated. See Appendix C.2 for more details.

Given a single contrast hypothesis H_{0k} and population treatment assignment $z \in \{0, 1\}^N$, the *active focal units* of a module \mathcal{S} are the eligible focal units that are exposed to the levels defined in the null hypothesis H_{0k} , namely

$$\mathbf{A}_{\text{foc}}(z; \mathcal{S}) := \left\{ i \in \mathbf{E}_{\text{foc}}(\mathcal{S}) : z_i = 0 \text{ and } w_i(z) \in \{w_k, w_{k+1}\} \right\}. \quad (10)$$

A module \mathcal{S} is *active* under treatment z if $\mathbf{A}_{\text{foc}}(z; \mathcal{S}) \neq \emptyset$. Similarly, we define the *active randomization units* of \mathcal{S} as $\mathbf{A}_{\text{rand}}(z; \mathcal{S}) := \mathcal{N}(\mathbf{A}_{\text{foc}}(z; \mathcal{S})) \subseteq \mathbf{E}_{\text{rand}}(\mathcal{S})$.

These definitions are illustrated in Figure 2 as a continuation of Figure 1 under an

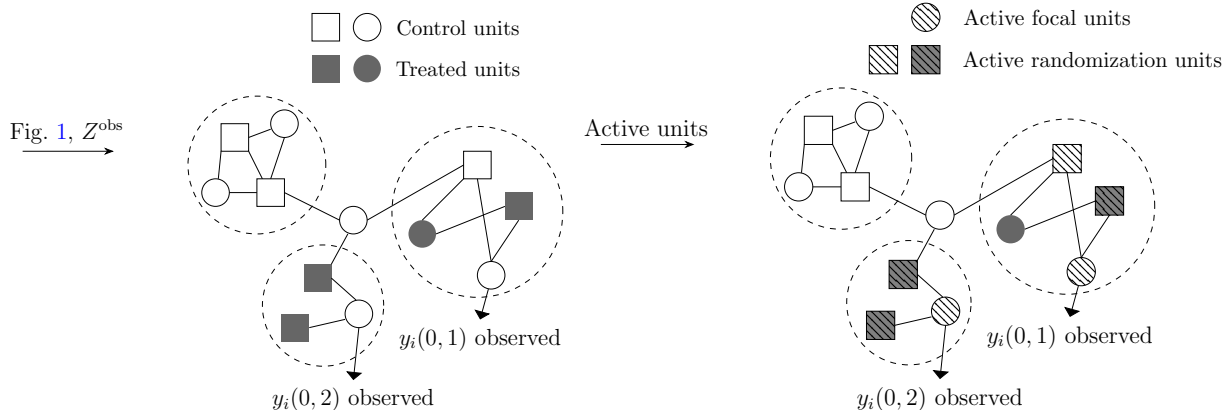


Figure 2: Continuing from Figure 1. *Left panel:* Z^{obs} is realized. Shaded color indicates treated units. *Right panel:* Nodes with hatched pattern represent active focal/randomization units for the null hypothesis $H_{0k} : y_i(0, 1) \geq y_i(0, 2)$.

observed treatment assignment Z^{obs} with $w_k = 1$ and $w_{k+1} = 2$, indicating 1 and 2 treated neighbors respectively. Shaded circles and squares are treated under Z^{obs} . The module in the upper left panel is not active since, under Z^{obs} , the eligible focal units in it have no neighbor treated. In the upper right module, only one eligible focal unit becomes active since the other focal unit is itself treated ($Z_i^{\text{obs}} = 1$). The module in the bottom is active as well since the eligible focal unit has 2 neighbors treated.

We are now ready to define the testing procedure for the single contrast hypothesis H_{0k} .

4.2 Testing a single contrast hypothesis, H_{0k}

To build intuition, we first present Algorithm 1 that describes in detail the steps for testing H_{0k} assuming that each module in our analysis is uniform. As we will see, the use of uniform modules simplifies the randomization distribution to a simple (clustered) Bernoulli randomization, as if we were randomizing the exposures w_k, w_{k+1} on the active focal units of each module.

The first step of Algorithm 1 (Lines 1-2) is to find the active focal and active randomization units under Z^{obs} , which define the set of active modules denoted by \mathcal{L}^{obs} . Note that \mathcal{L}^{obs} depends on the observed Z^{obs} , and is thus a random variable. Lines 3-6 calculate the

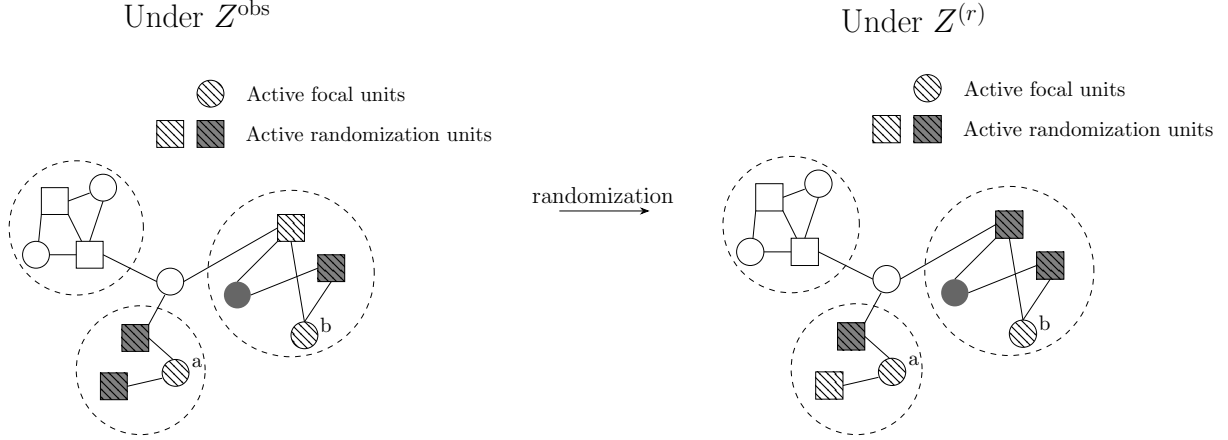


Figure 3: Illustration of Algorithm 1 in testing $H_{0k} : y_i(0, 1) \geq y_i(0, 2)$. *Left panel:* The observed outcome for node “a” is $Y_a^{\text{obs}} = y_a(0, 2)$ and the observed outcome for node “b” is $Y_b^{\text{obs}} = y_b(0, 1)$. *Right panel:* The randomized treatment $Z^{(r)}$ happens to permute the treatments of the active modules (containing nodes “a” and “b”). Under this randomization, the exposures of the two active focal units “a” and “b” are permuted as well.

distributions of exposures on active focal units conditional on \mathcal{L}^{obs} being the set of active modules. Specifically, p_ℓ in Line 5 calculates the probability that units in $A_{\text{foc}}(Z^{\text{obs}}; \mathcal{S}_\ell)$ are exposed to w_{k+1} conditional on \mathcal{S}_ℓ being active. Finally, Lines 7-14 define the main randomization test that “shuffles” the exposures $\{w_k, w_{k+1}\}$ on the active focal units. Akin to cluster randomization, this can be simply implemented by, first, performing a Bernoulli randomization on the module level using the probabilities p_ℓ (Line 10), and then jointly setting the exposures of all focal units in each module according to that Bernoulli randomization (Line 11). We defer the proof of validity to Theorem 1 below.

An illustration of Algorithm 1 is shown in Figure 3, which continues the setup introduced earlier in Figure 2. The right panel shows a possible randomized treatment, $Z^{(r)}$ (Lines 8-12). The ι_ℓ from the Bernoulli randomization in Line 10 is realized to be 1 for the right upper module, while realized to be 0 for the bottom module. Hence, the active focal unit “b” is exposed to 2 treated neighbors while the active focal unit “a” is exposed to 1 treated neighbor. The resulting randomized treatment $Z^{(r)}$ permutes the exposures of node “a” and “b” under Z^{obs} . If, for example, the difference-in-means test statistic (7) is used with both ψ_1 and ψ_0 being the identity function, then $T^{\text{obs}} = Y_a^{\text{obs}} - Y_b^{\text{obs}}$ and $T^{(r)} = Y_b^{\text{obs}} - Y_a^{\text{obs}}$.

Algorithm 1 Test for single contrast hypothesis, $H_{0k} : y_i(0, w_k) \geq y_i(0, w_{k+1})$, assuming uniform modules

Require: Module set $\mathbb{S} = \{\mathcal{S}_1, \dots, \mathcal{S}_L\}$ such that each $\mathcal{S} \in \mathbb{S}$ is a uniform module; observed treatment Z^{obs} ; observed outcome Y^{obs} (Input).

Output: Finite-sample valid p -value for H_{0k} , pval_k .

// Preprocessing

- 1: Given Z^{obs} , calculate $\mathbf{A}_{\text{foc}}(Z^{\text{obs}}; \mathcal{S}_\ell)$ and $\mathbf{A}_{\text{rand}}(Z^{\text{obs}}; \mathcal{S}_\ell)$ for each $\ell \in [L]$ from Equation (10). Define the active module set $\mathcal{L}^{\text{obs}} = \{\ell \in [L] : \mathbf{A}_{\text{foc}}(Z^{\text{obs}}; \mathcal{S}_\ell) \neq \emptyset\}$ and the set of active focal units $\mathcal{U}^{\text{obs}} = \bigcup_{\ell \in [L]} \mathbf{A}_{\text{foc}}(Z^{\text{obs}}; \mathcal{S}_\ell)$.
- 2: Define an exposure-monotone test statistic in the order (w_k, w_{k+1}) ; e.g., difference-in-means as in Equation (7) as $t_k(z, y) := t_{w_k, w_{k+1}}^{\text{DIM}}(z, y; \mathcal{U}^{\text{obs}})$. Calculate the observed value of the test statistic $T^{\text{obs}} = t_k(Z^{\text{obs}}, Y^{\text{obs}})$.

// Calculate the conditional randomization distribution on active modules

- 3: **for** $\ell \in \mathcal{L}^{\text{obs}}$ **do**
- 4: Define $\mathcal{T}_\ell(w) = \{z_A \in \{0, 1\}^{|\mathbf{A}|} : w_i(z_A) = w, \forall i \in \mathbf{A}_{\text{foc}}(Z^{\text{obs}}; \mathcal{S}_\ell)\}$, for $w \in \{w_k, w_{k+1}\}$, where $\mathbf{A} = \mathbf{A}_{\text{rand}}(Z^{\text{obs}}; \mathcal{S}_\ell)$.
- 5: Calculate

$$p_{0\ell} = \sum_{z \in \mathcal{T}_\ell(w_k)} \prod_{j \in \mathbf{A}_{\text{rand}}(Z^{\text{obs}}; \mathcal{S}_\ell)} p_j^{z_j} (1 - p_j)^{1 - z_j}, \quad p_{1\ell} = \sum_{z \in \mathcal{T}_\ell(w_{k+1})} \prod_{j \in \mathbf{A}_{\text{rand}}(Z^{\text{obs}}; \mathcal{S}_\ell)} p_j^{z_j} (1 - p_j)^{1 - z_j},$$

and $p_\ell = p_{1\ell} / (p_{0\ell} + p_{1\ell})$.

- 6: **end for**

// Main randomization test

- 7: **for** $r = 1, \dots, R$ **do**
- 8: $Z^{(r)} \leftarrow Z^{\text{obs}}$.
- 9: **for** $\ell \in \mathcal{L}^{\text{obs}}$ **do**
- 10: Sample $\iota_\ell \sim \text{Bern}(p_\ell)$.
- 11: If $\iota_\ell = 1$, then sample $\tilde{Z}_\ell \sim \text{Unif}\{\mathcal{T}_\ell(w_{k+1})\}$; otherwise sample $\tilde{Z}_\ell \sim \text{Unif}\{\mathcal{T}_\ell(w_k)\}$. Update $Z_i^{(r)} \leftarrow \tilde{Z}_i$ for all $i \in \mathbf{A}_{\text{rand}}(Z^{\text{obs}}; \mathcal{S}_\ell)$.
- 12: **end for**
- 13: Calculate $T^{(r)} = t_k(Z^{(r)}, Y^{\text{obs}})$.
- 14: **end for**
- 15: Output p -value:

$$\text{pval}_k = \frac{1}{1 + R} \left(1 + \sum_{r=1}^R \mathbb{1}\{T^{(r)} \geq T^{\text{obs}}\} \right). \quad (11)$$

4.2.1 Extensions of Algorithm 1

Before moving to test the full monotone hypothesis, here we discuss some extensions of Algorithm 1. Further extensions to more general exposure functions and designs are presented in Appendix C.1.

Allowing non-uniform modules. It is straightforward to lift the requirement of uniform modules in Algorithm 1, and thus allow eligible focal units to have different neighbors. The main challenge with such an extension is that the exposures of active focal units in the same module may not take the same value, as opposed to Lines 4-5 and 10-11 of Algorithm 1. Instead, the randomization distribution for \tilde{Z}_ℓ is the conditional distribution of the non-uniform Bernoulli design P on $\mathbf{A} = \mathbf{A}_{\text{rand}}(Z^{\text{obs}}; \mathcal{S}_\ell)$ conditional on being in the set

$$\{z_{\mathbf{A}} \in \{0, 1\}^{|\mathbf{A}|} : w_i(z_{\mathbf{A}}) \in \{w_k, w_{k+1}\}, \forall i \in \mathbf{A}_{\text{foc}}(Z^{\text{obs}}; \mathcal{S}_\ell)\}. \quad (12)$$

This set can be enumerated whenever the space of active randomization units, namely $|\mathbf{A}_{\text{rand}}(Z^{\text{obs}}; \mathcal{S}_\ell)|$, is not too large. Alternatively, we could use rejection sampling or similar schemes to approximate the randomization distribution to arbitrary precision. Note also that (12) allows for other exposure functions apart from (2) as long as the exposure depends only on the treatments of a unit’s neighbors.

Choice of module set. Algorithm 1 gives a finite-sample valid test for any (uniform) module set, but does not specify which module set to use. Based on Theorem 3 in Puelz et al. (2022), which shows that the power of a conditional randomization test increases with both the number of focal units and the support of the conditional randomization distribution, it is better to choose a module set that gives more active focal units. However, we cannot simply maximize the observed number of active focal units under Z^{obs} , as this could raise selective inference problems. Instead, one valid approach would be to maximize the *expected* number of active focal units with respect to the design from which Z^{obs} is sampled, either through

exact calculations or Monte-Carlo.

4.3 Testing the full monotone hypothesis, H_0

Here we present our randomization test for the full monotone hypothesis H_0 in (3) under non-uniform Bernoulli designs. To build intuition, we begin with a simple procedure that splits the network “far enough” to eliminate dependence between p -values. We will then follow up with a more sophisticated procedure that takes the network structure into account.

A simple testing procedure. The p -value from Algorithm 1 is valid for testing the single contrast hypothesis H_{0k} . Thus, a straightforward way to test the full monotone null hypothesis H_0 is to, first, construct $K - 1$ non-overlapping module sets $\mathbb{S}_k = \{\mathcal{S}_{k,\ell} : \ell \in [L_k]\}$ for $k = 1, \dots, K - 1$, such that $\mathcal{S}_{k,\ell} \cap \mathcal{S}_{k',\ell'} = \emptyset$ for all $k \neq k'$, $\ell \in [L_k]$ and $\ell' \in [L_{k'}]$. Then, we test each contrast H_{0k} by Algorithm 1 applied on \mathbb{S}_k and get pval_k . Since pval_k is only a function of data from the module set \mathbb{S}_k , these p -values are mutually independent under a non-uniform Bernoulli design, and can thus be combined easily into a valid p -value for H_0 . While this approach is conceptually simple, the obvious downside is that we may discard too much network information to construct non-overlapping sub-networks.

A flexible testing procedure. A more flexible approach is to split the network in a way that allows possibly overlapping sub-networks inspired by Lemma 1. The idea is to split the network sequentially from $k = 1$ to $K - 1$, where at each step k we allow \mathbb{S}_k to have eligible randomization units that overlap with previous sub-networks. Reflecting this change, the randomization test on \mathbb{S}_k would need to be adapted by conditioning on treatments of all previously constructed sub-networks at their observed values under Z^{obs} .

This adaptation of the randomization test requires a small extension of Algorithm 1 to allow conditioning on the treatments of certain units. This is presented in Algorithm 1' that takes a set of units C as input on which the randomization test is conditioned (Line 3),

Algorithm 1' General test for single contrast hypothesis, $H_{0k} : y_i(0, w_k) \geq y_i(0, w_{k+1})$

Require: Module set $\mathbb{S} = \{\mathcal{S}_1, \dots, \mathcal{S}_L\}$; Z^{obs} ; Y^{obs} ; conditional set C (Input).

Output: Finite-sample valid p -value for H_{0k} , pval_k .

// Preprocessing

1: Same as Algorithm 1.

// Calculate conditional randomization distribution on active modules

2: **for** $\ell \in \mathcal{L}^{\text{obs}}$ **do**

3: Calculate the randomization distribution for active randomization units supported on $\{0, 1\}^{|\mathbf{A}_\ell|}$ where $\mathbf{A} = \mathbf{A}_{\text{rand}}(Z^{\text{obs}}; \mathcal{S}_\ell)$, conditional on treatment status of units in C :

$$r_{\ell,k}(z_{\mathbf{A}}) \propto \mathbb{1}\{w_i(z_{\mathbf{A}}) \in \{w_k, w_{k+1}\}, \forall i \in \mathbf{A}_{\text{foc}}(Z^{\text{obs}}; \mathcal{S}_\ell)\} P_\ell(z_{\mathbf{A}}|C), \quad (13)$$

where under the non-uniform Bernoulli design

$$P_\ell(z_{\mathbf{A}}|C) \propto \mathbb{1}\{z_{\mathbf{A} \cap C} = Z_{\mathbf{A} \cap C}^{\text{obs}}\} \prod_{j \in \mathbf{A} \setminus C} p_j^{z_j} (1 - p_j)^{1 - z_j}.$$

4: **end for**

// Main randomization test

5: Same as Algorithm 1, except that Lines 10-11 are changed to sample \tilde{Z}_ℓ from $r_{\ell,k}(\cdot)$.

while allowing for non-uniform modules. To test full null H_0 , we can now apply Algorithm 1' sequentially to construct multiple p -values to be combined through Fisher's combination.

The procedure to test H_0 is shown in Algorithm 2, and can be described as follows. For each k , in Line 2, we first construct module set \mathbb{S}_k such that the eligible focal units for each module in \mathbb{S}_k do not overlap with previous modules in the set. Importantly, to achieve more power, we allow overlap between the eligible randomization units across module sets. That is, both eligible focal units and eligible randomization units built at step $k' < k$ can become eligible randomization units for the modules built at step k . The potential benefit in power is illustrated in the left panel of Figure 4, where the grey square (labeled as "c") is a treated eligible randomization unit from a module set in \mathbb{S}_1 that is re-used in the subsequent module set \mathbb{S}_2 as another eligible randomization unit. In contrast, under the simple procedure described above, this unit could not be included in \mathbb{S}_2 . Next, in Line 3 we apply the single contrast hypothesis test (Algorithm 1') on module set \mathbb{S}_k conditioning on the treatments in set $C = \mathbb{S}_{<k}$, the units in all constructed module sets prior to k . As a result, in the right panel of Figure 4, the randomization test conditions on unit "c" being treated. Finally,

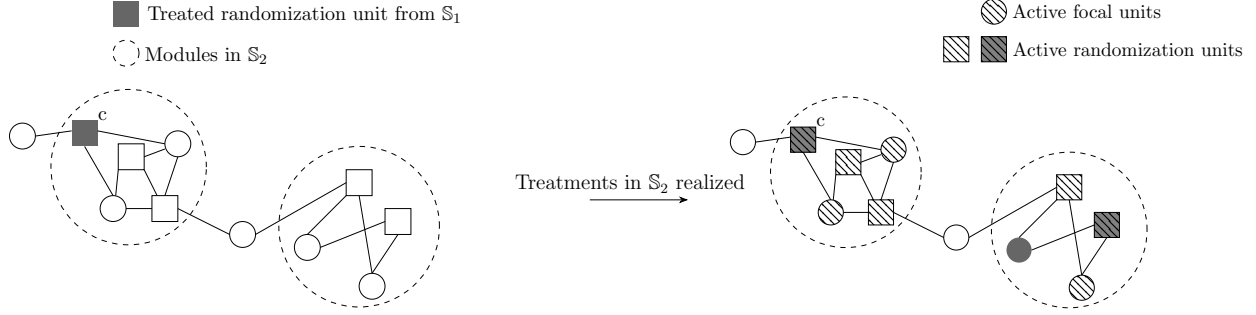


Figure 4: Illustration of Algorithm 2 showing overlap between module sets. *Left*: Each dashed circle represents a module in \mathbb{S}_2 , while the shaded square, labeled as “c”, is an eligible randomization unit that overlaps with those in \mathbb{S}_1 , and is realized to be treated. *Right*: Treatments in \mathbb{S}_2 are realized conditional on the treatments of \mathbb{S}_1 . The randomization test is then conditional on unit “c” being treated.

Algorithm 2 Test for monotone hypothesis, $H_0 : y_i(0, w_1) \geq y_i(0, w_2) \geq \dots \geq y_i(0, w_K)$

Require: Exposure set $\mathcal{W} = \{w_1, w_2, \dots, w_K\}$; observed treatment Z^{obs} ; observed outcome Y^{obs} (Input).

Output: Finite-sample valid p -value for H_0 , p_{FCT} .

- 1: **for** $k = 1, 2, \dots, K - 1$ **do**
 - 2: Construct module set $\mathbb{S}_k = \{\mathcal{S}_{k,1}, \dots, \mathcal{S}_{k,L_k}\}$ such that $E_{\text{foc}}(\mathcal{S}_{k,\ell}) \cap \mathbb{S}_{<k} = \emptyset$ for all $\ell \in [L_k]$, where $\mathbb{S}_{<k} := \bigcup_{k' < k} \bigcup_{\ell' \in [L_{k'}]} \mathcal{S}_{k',\ell'}$ with the convention $\mathbb{S}_{<1} := \emptyset$.
 - 3: Apply Algorithm 1' with module set \mathbb{S}_k , observed treatment Z^{obs} and outcome Y^{obs} , and conditional set $\mathbb{S}_{<k}$. Get p -value pval_k .
 - 4: **end for**
 - 5: Output the sequence of p -values $(\text{pval}_k)_{k=1}^{K-1}$ and the combined p -value p_{FCT} using (9).
-

Line 5 combines the p -values (pval_k) by Fisher’s rule to produce a valid p -value for the full monotone null, H_0 .

Theorem 1 below shows that these p -values are stochastically larger than uniform, and thus the combined p -value from Algorithm 2 leads to a finite-sample valid p -value for H_0 . The proof for this result is in Appendix A.

Theorem 1. *Suppose that the treatment assignment follows a non-uniform Bernoulli design in Definition 3. Then, each p -value from Algorithm 2, pval_k , is valid for $H_{0k} : y_i(0, w_k) \geq y_i(0, w_{k+1}) \forall i$. Moreover, these p -values are stochastically larger than uniform, and so the combined p -value from Line 5 of Algorithm 2 is valid under the monotone spillover hypothesis*

H_0 . Specifically,

$$\mathbb{P}(p_{\text{FCT}} \leq \alpha \mid H_0) \leq \alpha, \text{ for all } \alpha \in [0, 1],$$

where the probability is with respect to treatment randomization from the Bernoulli design.

Remark 1 (Covariate adjustment). At each step k in Algorithm 2, we can replace the outcome Y_i input into Algorithm 1' by $Y_i - \hat{f}_{k-1}(X_i)$ for all $i \in \bigcup_{\ell \in [L_k]} \mathcal{S}_{k,\ell}$, for some model \hat{f}_{k-1} fitted using data (Y_j^{obs}, X_j) for $j \in \mathbb{S}_{<k}$ only. For example, \hat{f}_{k-1} can be a linear regression of Y_j^{obs} on X_j using $j \in \mathbb{S}_{<k}$, or simply subtracting the pre-treatment baseline outcome Y_i^{pre} from Y_i^{obs} . The test remains valid because both \hat{f}_{k-1} and X_i does not change with Z_i^{obs} for $i \in \bigcup_{\ell \in [L_k]} \mathcal{S}_{k,\ell} \setminus \mathbb{S}_{<k}$ (recall that the randomization test at step k conditions on $Z_{\mathbb{S}_{<k}}^{\text{obs}}$), so that H_{0k} implies the monotonicity of the adjusted potential outcomes: $y_i(0, \mathbf{w}_k) - \hat{f}_{k-1}(X_i) \geq y_i(0, \mathbf{w}_{k+1}) - \hat{f}_{k-1}(X_i)$ for all $i \in \bigcup_{\ell \in [L_k]} \mathcal{S}_{k,\ell} \setminus \mathbb{S}_{<k}$.

Remark 2 (Comparison with previous literature). The result in Theorem 1 advances the growing literature of randomization tests under interference (Athey et al., 2018; Basse et al., 2019; Puelz et al., 2022). Prior methods cannot directly test monotone spillover hypotheses such as H_0 , and were mainly designed to test simpler null hypotheses of the form defined in Equation (5). Moreover, while methods like the ‘‘biclique method’’ of Puelz et al. (2022) can be adapted for testing monotone spillovers, they can be computationally demanding, particularly for large networks. We will discuss this in more detail in Section 5. Our method is also related to the one proposed in Zhang and Zhao (2024), which provides a general recipe for recursively constructing conditional randomization tests. Their method also builds on similar results to Rosenbaum (2011) as we do in Step 4 of Section 3. The key challenge in the recursive construction, however, is that it is context-specific. It remains unclear how this approach could be adapted to our monotone spillover hypothesis, where each individual hypothesis involves a contrast of exposure levels.

5 Methodology under Arbitrary Designs

The procedure outlined in Algorithm 2 relies heavily on the structure of the non-uniform Bernoulli design of Definition 3. In this section, we discuss how to test H_0 under an arbitrary experimental design $P(\cdot)$.

As before, we begin with a valid test for \tilde{H}_{0k} , which under general designs is possible through the biclique testing procedure of Puelz et al. (2022). Roughly speaking, this procedure translates a null hypothesis on treatment exposures into a bipartite graph —known as the “null exposure graph”— and conditions the randomization test on a biclique of this graph. The details are provided in Appendix D. Additionally, using similar arguments to Theorem 1, the biclique test will be valid for H_{0k} under an exposure-monotone test statistic.

With the biclique test for H_{0k} , we can test the full monotone null H_0 based on the idea of network splitting outlined in Section 3. Concretely, consider a partition of the network $\mathcal{G} = (V, E)$ into $\{\mathcal{G}_k\}_{k \in [K]}$, where $\mathcal{G}_k = (V_k, E_k)$, such that $V_k \cap V_{k'} = \emptyset$ for $k \neq k' \in [K]$. Then, we can conduct a biclique test of the null H_{0k} within sub-network \mathcal{G}_k , sequentially for $k = 1, 2, \dots, K - 1$, and combine the resulting p -values using Fisher’s combination rule. Importantly, in order to apply Lemma 1 and guarantee the validity of the combination, when testing H_{0k} on $\mathcal{G}_k = (V_k, E_k)$, we want to ensure that the exposure function $w_i(\cdot)$, for $i \in V_k$, is computable using only treatments of units in $V_{\leq k} := \bigcup_{k' \leq k} V_{k'}$, in the sense that $w_i(z) = w_i(z_{V_{\leq k}})$. Thus, before conducting the biclique test on \mathcal{G}_k , we may simply remove units in V_k whose exposures depend on treatments of units outside $V_{\leq k}$.

The partition of the network is not unique, however. Heuristically, the partition could aim to maximize the connections between nodes within each sub-network, and minimize the connections between nodes in different sub-networks. Several existing algorithms in the community detection literature work in this way, such as the Leiden algorithm in Traag et al. (2019). We discuss this algorithm in Appendix E and provide a way to select the partition based on statistics of null exposure graphs.

Given a choice of the partition, Algorithm 3 presents our proposed randomization test

Algorithm 3 Test for $H_0 : y_i(0, w_1) \geq y_i(0, w_2) \geq \dots \geq y_i(0, w_K)$ under general design.

Require: Exposure set $\mathcal{W} = \{w_1, w_2, \dots, w_K\}$; network \mathcal{G} and a partition $\{\mathcal{G}_k\}_{k \in [K]}$ with $\mathcal{G}_k = (V_k, E_k)$; design $P(\cdot)$; observed treatment Z^{obs} (Input).

Output: Finite-sample valid p -value for H_0 , p_{FCT} .

- 1: **for** $k = 1, 2, \dots, K - 1$ **do**
 - 2: Define $V'_k \leftarrow \{i \in V_k : w_i(z) \text{ is computable with } (z_i : i \in V_{\leq k})\}$.
 - 3: Run the biclique test on V'_k , using as input (i) the conditional distribution of Z_{V_k} given $(Z_i^{\text{obs}})_{i \in V_{<k}}$ where $V_{<k} := \bigcup_{k' < k} V_{k'}$, denoted as $P_k(\cdot)$; and (ii) an exposure-monotone test statistic t_k in the order (w_k, w_{k+1}) .
 - 4: From the biclique test above, obtain the biclique decomposition $\{\mathcal{C}_j^k\}_{j \in J_k}$ (defined in Appendix D) and the corresponding p -value pval_k .
 - 5: **end for**
 - 6: Output the sequence of p -values $(\text{pval}_k)_{k=1}^{K-1}$ and the combined p -value p_{FCT} using (9).
-

for the monotone null H_0 under a general design $P(\cdot)$. The validity of the algorithm is given in Theorem 2 that follows. The proof is presented in Appendix A.

Theorem 2. For any $k \in [K - 1]$ and $\alpha_k \in [0, 1]$ in Algorithm 3,

$$\mathbb{P}_{Z_{V_k}^{\text{obs}} \sim P_k(\cdot)} \left(\text{pval}_k \leq \alpha_k \mid \{\mathcal{C}_j^k\}_{j \in J_k}, (Z_i^{\text{obs}})_{i \in V_{<k}}, H_{0k} \right) \leq \alpha_k,$$

where $P_k(\cdot)$ is defined in Line 3 of Algorithm 3 as $P_k(Z_{V_k}) = P(Z_{V_k} | Z_{V_{<k}}^{\text{obs}})$. Moreover, the p -values $(\text{pval}_k)_k$ are stochastically larger than uniform, so the combined p -value from Line 6 of Algorithm 3 is valid under the monotone spillover hypothesis H_0 . That is, $\mathbb{P}(p_{\text{FCT}} \leq \alpha \mid H_0) \leq \alpha$ for all $\alpha \in [0, 1]$, where the probability is taken with respect to design the $P(\cdot)$.

Algorithm 3 can handle general designs but could be computationally intensive. The main computational challenge is to build the null exposure graph and execute the biclique test based on the conditional distribution specified recursively in Line 3. When the treatment follows a non-uniform Bernoulli design as in Section 4, this conditional distribution is still a non-uniform Bernoulli design on the set V_k and is computationally easy to sample from to build the null exposure graph. Similarly, this conditional distribution has a simple structure whenever the experiment follows a completely randomized design, or a clustered or blocked completely randomized design. Under general designs, however, the form of this conditional distribution may be complex. On the other hand, under the non-uniform Bernoulli

design, the module-based test in Section 4 is significantly easier computationally compared to the biclique-based test and can also achieve higher power as shown in the simulations in Section 6.3 and Appendix E.3 below, by leveraging the structure of the design.

6 Simulated Studies: Validity and Power

In this section, we examine our methods in simulations. We will use as a basis a large-scale “hotspots” policing experiment in Medellín, Colombia conducted by Collazos et al. (2021) to test a monotone spillover hypothesis related to the crime displacement hypothesis discussed in Example 1. First, we describe some background information on the experiment, and then demonstrate our randomization procedures using both simulated and real outcomes.

6.1 Background

The units of the experiment were $N = 37,055$ street segments in Medellín. Based on past crime data and input from the police, 967 of them were selected as “hotspot” streets. Among these hotspots, 384 were randomly assigned to treatment consisting of a 50-80% increase in police patrol time over a period of six months. Treatment assignment was subject to certain complex constraints imposed by the police.³ To simplify, we approximate the design through a non-uniform Bernoulli design with unit treatment probabilities calculated from the true assignment mechanism. We think this approximation is adequate as the unit-level treatments according to the true assignment mechanism are uncorrelated.

The outcomes of interest are post-treatment crime counts on five types of crime: homicides, assaults, car theft, motorbike theft, and personal robbery, as well as a crime index weighted by the relative average prison sentence.⁴ Crime spillovers of any type are possible due to the adjacency between nearby streets. Let $d(i, j)$ denote the distance between two

³For instance, the police limited the number of treated hotspots across policing stations. Moreover, due to an inadvertent coding error, 7 hotspots were always assigned to treatment (Collazos et al., 2021).

⁴0.550 for homicides, 0.112 for assaults, 0.221 for car and motorbike theft, and 0.116 for robbery.

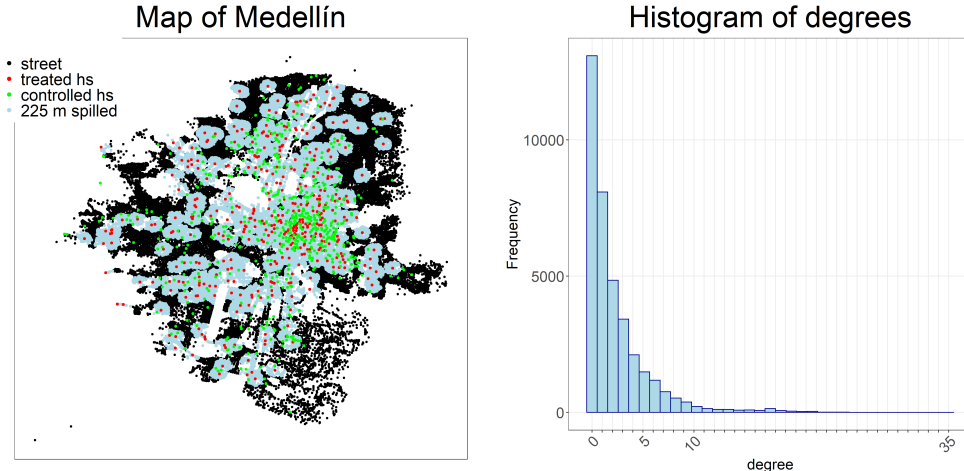


Figure 5: Map of Medellín and histogram of degrees for all units.

streets i and j , defined as the geographic distance between their midpoints. We consider the following treatment exposure function akin to the definition in Equation (2):

$$w_i(z) = \sum_{j \in \mathcal{N}_i} z_j, \quad \mathcal{N}_i = \{j \in [N] : d(i, j) \leq r\}.$$

This definition counts how many streets that are neighbors of street i are treated, where a neighbor of i is any street within r meters of i . We choose $r = 225$, following the analysis in Collazos et al. (2021); Puelz et al. (2022). Figure 5 (left panel) shows the geography of Medellín and the arrangement of treated and control hotspot streets as they were observed in the actual experiment. The right panel shows a histogram of the number of neighboring hotspot streets (we call them as “degree”) across all streets, revealing a pattern typically found in scale-free networks (Kolaczyk, 2009).

Based on these observations, we define $\mathcal{W} = \{0, 1, 2, [\geq 3]\}$ as the set of possible exposures, where “[≥ 3]” denotes any exposure with at least 3 treated neighbors. That is, all units with $w_i \geq 3$ are grouped into one exposure category labeled as “[≥ 3]”. Under Assumption 1, this implies that the controlled potential outcomes of a street are the same for all exposures that include at least 3 treated neighbors. This assumption is limiting but it simplifies the analysis and can be justified through an empirical evaluation using randomization tests; see Appendix F.1 for details. Moreover, to check the robustness of our results, in Appendix F.4

we consider an alternate definition of the exposure set, $\mathcal{W} = \{0, 1, 2, 3, 4, [\geq 5]\}$, where “[≥ 5]” is defined similarly and allows for more exposure levels.

Given the exposure set, we consider the following monotone null hypothesis:

$$H_0 = \bigcap_{k \in [3]} H_{0k}, \text{ where} \tag{14}$$

$$H_{01} : y_i(0, 0) \geq y_i(0, 1), \quad H_{02} : y_i(0, 1) \geq y_i(0, 2), \quad H_{03} : y_i(0, 2) \geq y_i(0, [\geq 3]), \quad \forall i.$$

The potential outcome $y_i(0, w)$ represents a certain crime occurrence when i is in control and receives exposure w . That is, we are testing the hypothesis that a street is benefited from having treated neighbor streets, and that this benefit is weakly monotonic. In the real data analysis of Section 7, we will also consider the above hypothesis in the opposite direction:

$$H'_0 = \bigcap_{k \in [3]} H'_{0k}, \text{ where} \tag{15}$$

$$H'_{01} : y_i(0, 0) \leq y_i(0, 1), \quad H'_{02} : y_i(0, 1) \leq y_i(0, 2), \quad H'_{03} : y_i(0, 2) \leq y_i(0, [\geq 3]), \quad \forall i.$$

This hypothesis formulates the crime displacement hypothesis: a street is negatively impacted from having treated neighbor streets, and the impact is weakly monotonic. We note that a rejection of an individual hypothesis H_{0k} implies a non-rejection of H'_{0k} . However, this need not be true for the combined hypotheses, H_0 and H'_0 , since the combination typically involves a non-linear transformation of individual p -values.

6.2 Simulation DGPs

We consider four different data generating processes (DGP) for the monotone hypothesis (14), each showcasing a particular aspect of our proposed methodology. For each DGP, the control potential outcomes are generated as $y_i(0, 0) \stackrel{iid}{\sim} \text{Gamma}(\hat{\alpha}, \hat{\beta})$, where $(\hat{\alpha}, \hat{\beta})$ are calibrated on the real Medellín data by matching the mean and variance of the observed post-treatment crime index among units that are in control ($Z_i^{\text{obs}} = 0$) and receive no exposure,

i.e., $w_i(Z^{\text{obs}}) = 0$. The remaining potential outcomes are defined as follows.

$$y_i(z_i, w_i) = y_i(0, 0) \exp\{-z_i + \tau w_i(1 - 0.5z_i)\}, \quad (\text{DGP1})$$

$$y_i(z_i, w_i) = y_i(0, 0) \exp\{-z_i + \tau[w_i - 2\mathbb{1}(w_i = 1)](1 - 0.5z_i)\}, \quad (\text{DGP2})$$

$$y_i(z_i, w_i) = y_i(0, 0) \exp\{-z_i + \tau w_i \cdot (1 - 0.5z_i) + \theta d_i\}, \quad (\text{DGP3})$$

$$y_i(z_i, w_i) = y_i^*(0, 0) \exp\{-z_i + \tau w_i(1 - 0.5z_i)\}, \quad (\text{DGP4})$$

$$\text{with } y_i^*(0, 0) = y_i(0, 0) + \frac{|G_{i,\varepsilon}^{r'}|}{\sqrt{\sum_j G_{i,j}^r}}, \quad \varepsilon_i \stackrel{iid}{\sim} N(0, 1).$$

DGP1 is used to illustrate the validity of our approach for $\tau \leq 0$, and its power against $\tau > 0$. DGP2 is a variation of DGP1 with heterogeneity and non-monotonicity in the spillover effect. Specifically, when $\tau > 0$, the spillover effect turns from positive to negative when $w_i = 1$ for control streets, and reverses for treated streets. DGP3 introduces network-related confounding where the degree d_i of street i affects outcomes at a level controlled by parameter θ . DGP4 introduces confounding through network-correlated errors, where $G^r \in \{0, 1\}^{N \times N}$ with $G_{i,j}^r = \mathbb{1}\{d(i, j) \leq r\}$ as its (i, j) -th element and $G_{i,\cdot}^r$ as its i -th row.

For test statistics in the randomization tests, we consider the simple difference-in-means (“DiM”) defined in (7) and the Stephenson rank sum statistics defined in (8) with $\varphi(r) = \binom{r-1}{s-1}$ if $r \geq s$ and $\varphi(r) = 0$ otherwise, for $s = 5, 20$. We refer to these as “rs5” and “rs20”, respectively. Apart from Fisher’s combination of p -values, we also consider Stouffer’s combination $p_{\text{Stouf}} = \Phi(\sum_k n_k \Phi^{-1}(p_k) / \|n\|_2)$, where $\Phi(\cdot)$ denotes the standard Normal CDF, and $n = (n_1, n_2, n_3)$ with n_k being the number of active focal units for $k = 1, 2, 3$. Additionally, as a baseline procedure, we consider a one-sided \mathfrak{t} -test on the coefficient on w_i in the linear regression model of $\log Y_i$ on treatment Z_i , exposure w_i and their interaction $Z_i \cdot w_i$.

6.3 Simulation results

The simulation results for all DGPs are presented in Table 1. The results are calculated over 2,000 replications, corresponding to a $\pm 0.5\%$ sampling error. In DGP1, we see that

all methods are valid, including the baseline OLS procedure. The rank sum statistics is generally low-powered, partly due to homogeneity in the effects, but the difference-in-means test statistic leads to a randomization test with a power comparable to OLS (roughly 70%). The Fisher and Stouffer combination rules differ only slightly.

In DGP2, our randomization tests are all valid in the absence of spillover effect ($\tau = 0$). In contrast to DGP1, settings with negative τ lead to a violation of the monotonicity hypothesis as well. We see that the randomization tests with the difference-in-means statistic are powerful against these alternatives, whereas OLS is not. The randomization test with the rank-sum statistic is again low-powered but is clearly better compared to OLS against those alternatives. Interestingly, there is a noticeable difference between the Fisher and Stouffer combination rules in terms of power under DGP2, due to the behavior of the transformation $\Phi^{-1}(p)$ when $p \rightarrow 0$ and 1. We discuss more about this issue in Appendix B.

In DGP3 and DGP4, we fix $\tau = 0$ (no spillover effect) and vary the degree of network confounding through parameters θ and r , respectively. We therefore expect all valid procedures to reject at 5% across all these simulations. Indeed, the randomization-based tests are all valid across all settings and combination rules. However, the OLS-based tests are significantly distorted. For instance, in DGP3, the OLS test over-rejects at a level 94% when $\theta = 0.1$. An increasing θ parameter leads to a spurious correlation between outcomes and network degree, which confounds OLS. In DGP4, OLS over-rejects from 13.9% to 38.50% as we increase r from 50 to 400. An increasing parameter r leads to an increasingly long-range correlation between error terms in the potential outcomes, leading in turn to a spurious correlation between observed outcomes and network treatment exposure. See Appendix F.2 for additional empirical evidence.

Remark 3. One can also run a regression saturated at both treatment and exposure, i.e., $Y_i = \sum_{z \in \{0,1\}} \sum_{k \in [K]} \mathbb{1}\{Z_i = z, w_i = w_k\} \beta_{z,k} + \varepsilon_i$, and test the monotone hypothesis (14) by testing $\beta_{0,k} \geq \beta_{0,k'} \forall k \leq k'$ using the limiting distribution of $\widehat{\beta}_{z,k}$. The validity of this approach again depends critically on the correct specification of the model, without

Combination		Test statistic	Spillover effect τ							
			-0.5	-0.2	-0.1	0	0.1	0.2	0.5	
DGP1	Fisher	DiM	0.00	0.00	0.40	5.15	24.65	62.25	100.00	
		rs5	1.20	2.85	3.45	5.70	6.55	7.40	13.60	
		rs20	0.20	1.10	2.25	4.90	9.55	17.20	50.55	
	Stouffer	DiM	0.00	0.00	0.35	5.10	27.50	67.20	99.95	
		rs5	1.35	3.00	3.50	6.05	6.50	8.00	11.90	
		rs20	0.00	1.10	2.30	5.90	10.00	16.20	45.65	
	OLS		0.00	0.00	0.35	4.90	40.65	88.30	100.00	
	Combination			Spillover effect τ						
				-0.5	-0.2	-0.1	0	0.1	0.2	0.5
DGP2	Fisher	DiM	94.45	18.60	6.10	4.15	16.60	52.65	99.85	
		rs5	2.85	2.90	4.40	4.95	6.40	7.05	13.80	
		rs20	7.50	2.45	3.85	5.15	9.70	16.80	59.15	
	Stouffer	DiM	94.55	31.30	14.10	4.55	1.55	0.25	0.00	
		rs5	6.25	4.90	5.15	5.60	4.35	4.90	3.00	
		rs20	12.55	7.90	5.95	5.90	3.85	3.20	0.55	
	OLS		0.00	0.00	0.35	4.90	36.35	79.50	100.00	
	Combination			Degree confounding θ ($\tau = 0$ throughout)						
				-0.3	-0.2	-0.1	0	0.1	0.2	0.3
DGP3	Fisher	DiM	5.20	5.15	4.85	5.40	4.95	4.95	5.25	
		rs5	4.55	5.00	5.05	4.10	5.35	5.25	4.00	
		rs20	4.50	4.85	4.95	4.25	4.55	5.65	4.00	
	OLS		0.00	0.00	0.00	5.10	94.05	100.00	100.00	
	Combination		tstat	Network correlation r ($\tau = 0$ throughout)						
			0	50	100	150	225	350	400	
DGP4	Fisher	DiM	4.67	4.60	4.80	4.50	5.65	5.03	4.50	
		rs5	4.92	5.20	5.10	4.35	5.25	3.92	3.60	
		rs20	4.67	4.90	5.30	4.75	5.00	4.47	4.35	
	OLS		5.13	13.90	23.95	29.80	34.10	37.14	38.50	

Table 1: Simulation results for DGP1-DGP4 under 2,000 replications. All tests are conducted at the 5% level and the reported values are rejection probabilities (in %).

which the β does not represent the true causal effect (DGP3). Even under the correct specification, establishing the limiting distribution can also be challenging when, for example,

the correlation between outcomes is too strong, as in DGP4.

7 Application: Testing Monotonicity in Crime Spillovers

We now turn to testing the monotone nulls defined in Equations (14) and (15) using the real Medellín data, where we specify $\mathcal{W} = \{0, 1, 2, [\geq 3]\}$. The robustness results for the alternative specification $\mathcal{W} = \{0, 1, 2, 3, 4, [\geq 5]\}$ are presented in Appendix F.4.

The left panel of Figure 6 displays the histograms of the post-treatment counts of the five types of crime and the crime index. Generally, all these outcomes are inflated at zero, and some of them take a few large values. Also, many of the pre-treatment baseline outcomes are identical to the post-treatment ones. As a result, we adjust each outcome by its pre-treatment value and use the difference between post- and pre-treatment crime or crime index, $\Delta Y_i = Y_i^{\text{post}} - Y_i^{\text{pre}}$, as the (adjusted) outcome in test statistics. The histogram of ΔY_i is displayed in the right panel in Figure 6. For test statistics, we again use the difference-in-means and the rank sum statistics in Section 6.2. We pay particular attention to the rank sum statistics due to their ability to detect uncommon-but-dramatic responses to treatment and often superior power under treatment effect heterogeneity (Caughey et al., 2023), which could be useful for detecting the violation of individual-level monotonicity given the distribution of ΔY_i in our setting. For brevity, in the following we will focus on crime index as the outcome. Results for other outcomes are presented in Appendix F.3.

To account for the uncertainty in constructing module sets, we repeat the construction 2,000 times independently, run Algorithm 2 for each construction, and report twice the median of all the 2,000 p -values for (14) in the third column in Table 2, which is a valid but potentially conservative p -value.⁵ Figure 7 shows descriptive histograms of the numbers of eligible and active focal units across the 2,000 replications.

To get a sense of how the focal units are distributed on the city map, we display two

⁵See, for example, Lemma 4.1 in Chernozhukov et al. (2018). In Appendix F.3 we show the histograms of these p -values.

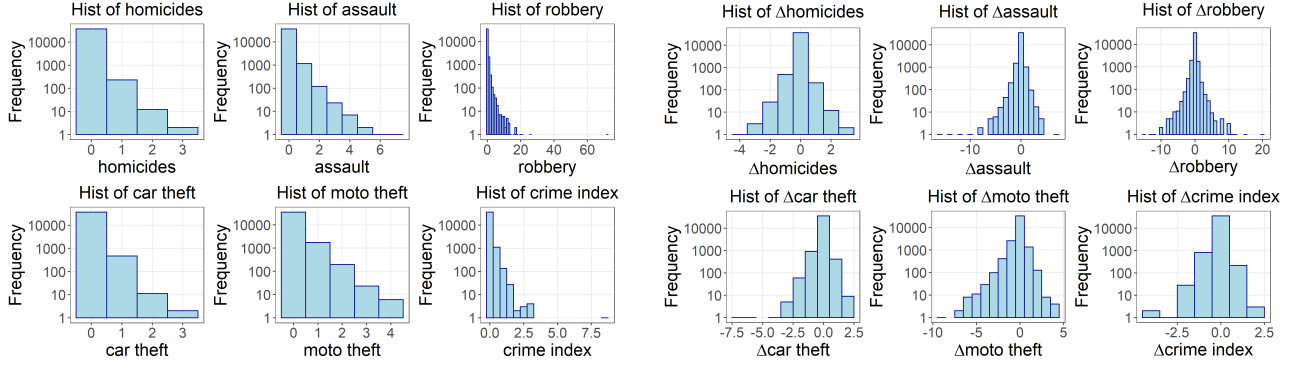


Figure 6: Histogram of crimes (left) and differences in post and pre treatment crimes (right).

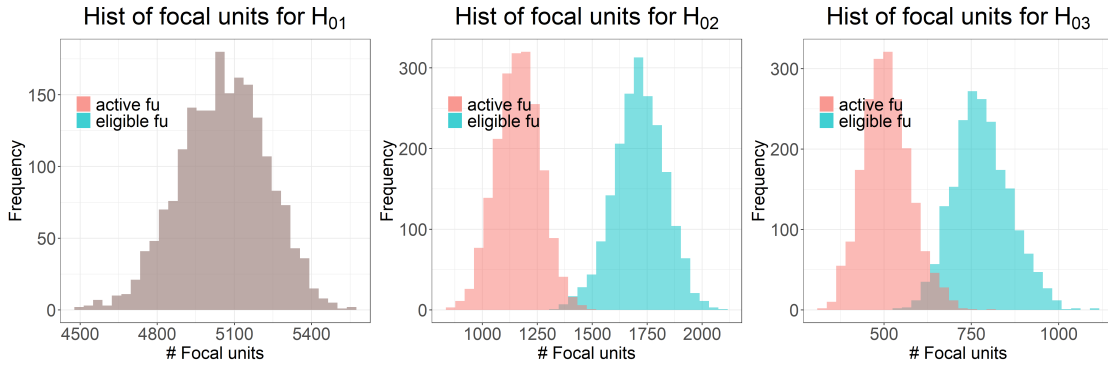


Figure 7: Histograms of number of focal units across the 2,000 constructions.

realizations of the algorithm in Figure 8. In general, there are far more eligible/active focal units for hypotheses involving lower level of exposures than for those involving higher levels. Also, focal units at lower exposure levels tend to be located at the outskirts of the city, while the focal units at higher exposure levels tend to be located at the center of the city. A plausible explanation for this observation is that there is higher density of hotspot streets at the city center, which is considered more disturbing, compared to the outskirts. We also apply the idea discussed in Section 4.2.1 to conduct tests on the module set that maximizes the expected number of active focal units among the 2,000 module sets, both for the beneficial hypothesis (14) and the crime displacement hypothesis (15). These results are presented in the fourth and fifth column of Table 2.

Overall, our randomization procedures consistently reject the beneficial spillover hypothesis (14) that the crime outcome is monotonically decreasing in the number of neighboring

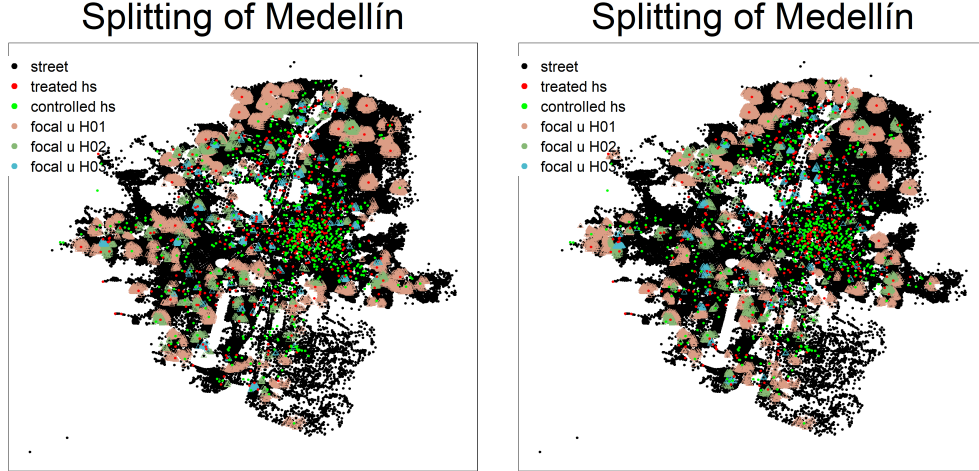


Figure 8: Two realizations of focal units for testing under exposures $\mathcal{W} = \{0, 1, 2, [\geq 3]\}$.

Hypothesis	test stat	Twice median	Max AFUs	Crime disp.
H_{01}	DiM	0.148	0.011	0.989
H_{02}		0.856	0.538	0.462
H_{03}		0.406	0.200	0.800
H_0 by FCT		0.179	0.036	0.919
H_{01}	rs5	0.074	0.008	0.992
H_{02}		0.128	0.055	0.945
H_{03}		0.404	0.182	0.818
H_0 by FCT		0.029	0.004	0.997
H_{01}	rs20	0.159	0.011	0.989
H_{02}		0.220	0.164	0.836
H_{03}		0.513	0.280	0.720
H_0 by FCT		0.095	0.019	0.984

Table 2: Third column: Twice the median of p -values for testing (14) across 2,000 module set constructions. Fourth column: p -values for testing (14) using the module sets that maximize the expected number of active focal units. Fifth column: p -values for testing the crime displacement hypothesis (15) using the module sets that maximize the expected number of active focal units. **Bold** denotes value below 0.05.

treated streets. Moreover, p -values tend to increase from H_{01} to H_{03} , and the strongest rejection signal comes from H_{01} , so that the failure of monotonicity mainly comes from the individual null hypothesis $H_{01} : y_i(0, 0) \geq y_i(0, 1)$. This suggests that there is negative crime spillover from nearby policing, supporting the crime displacement hypothesis which we fail to reject. However, our results also provide some evidence of “diminishing returns”, as more intense nearby policing may not necessarily lead to increased crime displacement.

8 Concluding remarks

In this paper, we extend randomization tests for spillover effects in network settings to test the monotonicity of spillover effects, leveraging the idea of network splitting and the “bounded null” perspective of randomization tests. An interesting future direction would be to study the power of our tests. Power analysis is particularly challenging in the current setup because it depends on the network topology, the alternative hypothesis, and the module set construction. Another valuable direction would be to formalize the test for diminishing returns of spillover effects. Although our current randomization tests can provide evidence for or against diminishing returns, they do not directly test the second derivative of the potential outcome function, which would be crucial for a formal test on diminishing returns.

References

- Aronow, P. M. and C. Samii (2017). Estimating average causal effects under general interference, with application to a social network experiment. *Annals of Applied Statistics* 11(4), 1912–1947.
- Athey, S., D. Eckles, and G. W. Imbens (2018). Exact p-values for network interference. *Journal of the American Statistical Association* 113(521), 230–240.
- Basse, G., P. Ding, A. Feller, and P. Toulis (2024). Randomization tests for peer effects in group formation experiments. *Econometrica* 92(2), 567–590.
- Basse, G. W., A. Feller, and P. Toulis (2019). Randomization tests of causal effects under interference. *Biometrika* 106(2), 487–494.
- Birnbaum, A. (1954). Combining independent tests of significance. *Journal of the American Statistical Association* 49(267), 559–574.
- Blattman, C., D. P. Green, D. Ortega, and S. Tobón (2021). Place-based interventions at scale: The direct and spillover effects of policing and city services on crime. *Journal of the European Economic Association* 19(4), 2022–2051.
- Brannath, W., M. Posch, and P. Bauer (2002). Recursive combination tests. *Journal of the American Statistical Association* 97(457), 236–244.
- Breza, E., F. C. Stanford, M. Alsan, B. Alsan, A. Banerjee, A. G. Chandrasekhar, S. Eichmeyer, T. Glushko, P. Goldsmith-Pinkham, K. Holland, et al. (2021). Effects of a large-scale social media advertising campaign on holiday travel and covid-19 infections: a cluster randomized controlled trial. *Nature medicine* 27(9), 1622–1628.

- Caughey, D., A. Dafoe, X. Li, and L. Miratrix (2023). Randomisation inference beyond the sharp null: bounded null hypotheses and quantiles of individual treatment effects. *Journal of the Royal Statistical Society Series B: Statistical Methodology*, qkad080.
- Chernozhukov, V., M. Demirer, E. Duflo, and I. Fernandez-Val (2018). Generic machine learning inference on heterogeneous treatment effects in randomized experiments, with an application to immunization in india. Technical report, National Bureau of Economic Research.
- Collazos, D., E. García, D. Mejía, D. Ortega, and S. Tobón (2021). Hot spots policing in a high-crime environment: An experimental evaluation in medellin. *Journal of Experimental Criminology* 17, 473–506.
- Cox, D. R. (1958). Planning of experiments.
- Fisher, R. A. (1935). *The Design of Experiments*. Oliver and Boyd.
- Guerette, R. T. and K. J. Bowers (2017). Assessing the extent of crime displacement and diffusion of benefits: A review of situational crime prevention evaluations. *Crime Opportunity Theories*, 529–566.
- Heumos, L., A. C. Schaar, C. Lance, A. Litinetskaya, F. Drost, L. Zappia, M. D. Lücken, D. C. Strobl, J. Henao, F. Curion, et al. (2023). Best practices for single-cell analysis across modalities. *Nature Reviews Genetics* 24(8), 550–572.
- Hong, G. and S. W. Raudenbush (2006). Evaluating kindergarten retention policy: A case study of causal inference for multilevel observational data. *Journal of the American Statistical Association* 101(475), 901–910.
- Kolaczyk, E. (2009). Statistical analysis of network data: Methods and models. *Springer Series In Statistics*, 386.
- Liu, Y. and J. Xie (2019). Cauchy combination test: a powerful test with analytic p-value calculation under arbitrary dependency structures. *Journal of the American Statistical Association*.
- Logan, A. P., P. M. LaCasse, and B. J. Lunday (2023). Social network analysis of twitter interactions: a directed multilayer network approach. *Social Network Analysis and Mining* 13(1), 65.
- Manski, C. F. (2013). Identification of treatment response with social interactions. *The Econometrics Journal* 16(1), S1–S23.
- Puelz, D., G. Basse, A. Feller, and P. Toulis (2022). A graph-theoretic approach to randomization tests of causal effects under general interference. *Journal of the Royal Statistical Society Series B: Statistical Methodology* 84(1), 174–204.
- Rosenbaum, P. R. (2011). Some approximate evidence factors in observational studies. *Journal of the American Statistical Association* 106(493), 285–295.

- Rubin, D. B. (1980). Randomization analysis of experimental data: The fisher randomization test comment. *Journal of the American statistical association* 75(371), 591–593.
- Stouffer, S. A., E. A. Suchman, L. C. DeVinney, S. A. Star, and R. M. Williams Jr (1949). The american soldier: Adjustment during army life.(studies in social psychology in world war ii), vol. 1.
- Traag, V. A., L. Waltman, and N. J. Van Eck (2019). From louvain to leiden: guaranteeing well-connected communities. *Scientific reports* 9(1), 5233.
- Zhang, Y., C. A. Phillips, G. L. Rogers, E. J. Baker, E. J. Chesler, and M. A. Langston (2014). On finding bicliques in bipartite graphs: a novel algorithm and its application to the integration of diverse biological data types. *BMC bioinformatics* 15, 1–18.
- Zhang, Y. and Q. Zhao (2024). Multiple conditional randomization tests for lagged and spillover treatment effects. *Biometrika*, asae042.

Supplementary Material

A Proof of results

A.1 Details of exposure monotone statistics

Verifying the exposure monotonicity follows from arguments similar to those in Proposition 1 and 2 of [Caughey et al. \(2023\)](#). Let $\eta_i \geq 0 \geq \xi_i$, $i \in \mathcal{U}$ and define $N_{z,w} = \sum_{i \in \mathcal{U}} I_i(z, w)$. To show that the difference-in-means statistic (7) satisfies the exposure-monotone property, note that

$$\begin{aligned} & t_{w,w'}^{\text{DiM}}(z, y_{\eta\xi}; \mathcal{C}) - t_{w,w'}^{\text{DiM}}(z, y; \mathcal{C}) \\ &= \sum_{i \in \mathcal{U}} \frac{I_i(z, w')}{N_{z,w'}} (\psi_1(y_i + \eta_i) - \psi_1(y_i)) - \sum_{i \in \mathcal{U}} \frac{I_i(z, w)}{N_{z,w}} (\psi_0(y_i + \xi_i) - \psi_0(y_i)) \geq 0, \end{aligned}$$

because both $\psi_1(\cdot)$ and $\psi_0(\cdot)$ are non-decreasing, as desired.

To show the rank-sum statistic (8) satisfies the exposure-monotone property, recall when there are ties we define the value of $\varphi(\cdot)$ to be the average of $\varphi(\cdot)$ evaluated at those ranks with ties broken by unit ordering, so it suffices to consider the ranks defined by

$$r_i(y_{\mathcal{U}}) = \sum_{j \in \mathcal{U}} \delta_{ij}(y_i, y_j), \quad \text{where } \delta_{ij}(y_i, y_j) = \mathbb{1}\{y_i > y_j\} + \mathbb{1}\{y_i = y_j, i \geq j\}.$$

The desired conclusion now follows from Lemma A3 in [Caughey et al. \(2023\)](#) by mapping our $(y_{\mathcal{U}}, \mathcal{U}, I_i(z, w'))$ to their $(\mathbf{y}, [n], \mathbb{1}\{z_i = 1\})$.

A.2 Proof of Theorem 1

Proof of Theorem 1. We will proceed the proof in three steps. Throughout $\{\mathbb{S}_k\}_k$ is considered fixed.

1. pval_k is valid for \tilde{H}_{0k} : We will apply ([Basse et al., 2019](#), Theorem 1). Under the non-

uniform Bernoulli design, it suffices to consider treatments within $\mathbb{S}_{\leq k}$. Given $\mathbb{S}_{\leq k}$, define

$$\mathbb{C}_k = \{(\mathcal{U}_k, \mathcal{Z}_k) : \mathcal{U}_k \subseteq \mathbb{S}_{\leq k}, \mathcal{Z}_k \subseteq \{0, 1\}^{|\mathbb{S}_{\leq k}|}\},$$

the space of ‘‘conditioning event’’ (Basse et al., 2019). The preprocessing step in Algorithm 1’ defines the following ‘‘conditioning mechanism’’ that maps any $Z_{\mathbb{S}_{\leq k}} \in \{0, 1\}^{|\mathbb{S}_{\leq k}|}$ into a (degenerate) distribution over \mathbb{C}_k :

$$m_k(\mathcal{U}_k, \mathcal{Z}_k | Z_{\mathbb{S}_{\leq k}}) = f_k(\mathcal{U}_k | Z_{\mathbb{S}_{\leq k}}) g_k(\mathcal{Z}_k | \mathcal{U}_k, Z_{\mathbb{S}_{\leq k}})$$

where

$$\begin{aligned} f_k(\mathcal{U}_k | Z_{\mathbb{S}_{\leq k}}) &= \mathbb{1}\left\{\mathcal{U}_k = \bigcup_{\ell \in [L_k]} \mathbf{A}_{\text{foc}}(Z_{\mathbb{S}_{\leq k}}; \mathcal{S}_{k, \ell})\right\} \\ &= \mathbb{1}\left\{\mathcal{U}_k = \left\{i \in \bigcup_{\ell \in [L_k]} \mathbf{E}_{\text{foc}}(\mathcal{S}_{k, \ell}) : Z_i = 0, w_i(Z_{\mathbb{S}_{\leq k}}) \in \{w_k, w_{k+1}\}\right\}\right\} \end{aligned}$$

$$g_k(\mathcal{Z}_k | \mathcal{U}_k, Z_{\mathbb{S}_{\leq k}})$$

$$= \mathbb{1}\left\{\mathcal{Z}_k = \left\{Z' \in \text{supp}(P) \cap \mathbb{S}_{\leq k} : Z'_{\mathbb{S}_{\leq k} \setminus (\mathcal{N}(\mathcal{U}_k) \setminus \mathbb{S}_{< k})} = Z_{\mathbb{S}_{\leq k} \setminus (\mathcal{N}(\mathcal{U}_k) \setminus \mathbb{S}_{< k})}, w_i(Z'_{\mathbb{S}_{\leq k}}) \in \{w_k, w_{k+1}\}, \forall i \in \mathcal{U}_k\right\}\right\}.$$

The test conditions on treatments $Z_{\mathbb{S}_{< k}}$ so we remove it from $\mathcal{N}(\mathcal{U}_k)$ in $\mathbb{S}_{\leq k} \setminus (\mathcal{N}(\mathcal{U}_k) \setminus \mathbb{S}_{< k}) = (\mathbb{S}_{\leq k} \setminus \mathcal{N}(\mathcal{U}_k)) \cup \mathbb{S}_{< k}$. Both $w_i(Z_{\mathbb{S}_{\leq k}})$ and $w_i(Z'_{\mathbb{S}_{\leq k}})$ are well-defined as long as $w_i(Z)$ depends only on treatments of \mathcal{N}_i , or treatments of any other set included in $\mathbf{E}_{\text{rand}}(\mathcal{S}_{k, \ell})$, since by construction these sets are included in $\mathbf{E}_{\text{rand}}(\mathcal{S}_{k, \ell}) \subseteq \mathbb{S}_k \subseteq \mathbb{S}_{\leq k}$ for all $i \in \mathbf{E}_{\text{foc}}(\mathcal{S}_{k, \ell})$. The potential outcomes relevant for \tilde{H}_{0k} , $\{y_i(0, w_k), y_i(0, w_{k+1})\}$, are imputable for each $i \in \mathcal{U}_k$ under any $Z_{\mathbb{S}_{\leq k}} \in \mathcal{Z}_k$ following the definitions. Since the test statistic is exposure-monotone so it uses only potential outcomes in \mathcal{U}_k , the test statistic is also imputable.

It remains to show that the randomization distribution in (13) coincides with $\mathbb{P}(Z_{\mathbb{S}_{\leq k}} | \mathcal{C}_k^{\text{obs}}) \propto m_k(\mathcal{C}_k^{\text{obs}} | Z_{\mathbb{S}_{\leq k}}) P(Z_{\mathbb{S}_{\leq k}})$ where $\mathcal{C}_k^{\text{obs}} = (\mathcal{U}_k^{\text{obs}}, \mathcal{Z}_k^{\text{obs}}) \sim m_k(\cdot | Z_{\mathbb{S}_{\leq k}}^{\text{obs}})$. That is, the proposed randomization distribution coincides with the conditional distribution of $Z_{\mathbb{S}_{\leq k}}$ induced by the conditioning mechanism and the design.

Given $Z_{\mathbb{S}_{\leq k}}^{\text{obs}}$ and the induced set of all active focal units $\mathbf{A}_{\text{foc}}(Z_{\mathbb{S}_{\leq k}}^{\text{obs}}; \mathbb{S}_k) := \bigcup_{\ell \in [L_k]} \mathbf{A}_{\text{foc}}(Z_{\mathbb{S}_{\leq k}}^{\text{obs}}; \mathcal{S}_{k, \ell})$ which equals $\mathcal{U}_k^{\text{obs}}$ almost surely, as well as the set of all active randomization units $\mathbf{A}_{\text{rand}}(Z_{\mathbb{S}_{\leq k}}^{\text{obs}}; \mathbb{S}_k) :=$

$\bigcup_{\ell \in [L_k]} \mathbf{A}_{\text{rand}}(Z_{\mathbb{S}_{\leq k}}^{\text{obs}}; \mathcal{S}_{k,\ell})$, the $r_{k,\ell}(\cdot)$ in (13) defines a distribution on all units in $\mathbb{S}_{\leq k}$ by

$$\begin{aligned} r_k(Z_{\mathbb{S}_{\leq k}} = z_{\mathbb{S}_{\leq k}}) &\propto \mathbb{1}\{z_i = Z_i^{\text{obs}}, \forall i \in \mathbb{S}_{\leq k} \setminus (\mathbf{A}_{\text{rand}}(Z_{\mathbb{S}_{\leq k}}^{\text{obs}}; \mathcal{S}_k) \setminus \mathbb{S}_{<k})\} \\ &\quad \times \mathbb{1}\{w_i(z_{\mathbb{S}_{\leq k}}) \in \{w_k, w_{k+1}\}, \forall i \in \mathbf{A}_{\text{foc}}(Z_{\mathbb{S}_{\leq k}}^{\text{obs}}; \mathcal{S}_k)\} \\ &\quad \times P(z_{\mathbb{S}_{\leq k}}). \end{aligned}$$

Hence, it suffices to show that the two indicators above defines the same conditioning mechanism as m_k . That is,

$$\begin{aligned} &\mathbb{1}\{z_i = Z_i^{\text{obs}}, \forall i \in \mathbb{S}_{\leq k} \setminus (\mathbf{A}_{\text{rand}}(Z_{\mathbb{S}_{\leq k}}^{\text{obs}}; \mathcal{S}_k) \setminus \mathbb{S}_{<k})\} \\ &\quad \times \mathbb{1}\{w_i(z_{\mathbb{S}_{\leq k}}) \in \{w_k, w_{k+1}\}, \forall i \in \mathbf{A}_{\text{foc}}(Z_{\mathbb{S}_{\leq k}}^{\text{obs}}; \mathcal{S}_k)\} \\ &= f_k(\mathcal{U}_k^{\text{obs}} | z_{\mathbb{S}_{\leq k}}) g_k(\mathcal{Z}_k^{\text{obs}} | \mathcal{U}_k^{\text{obs}}, z_{\mathbb{S}_{\leq k}}), \end{aligned} \tag{16}$$

almost surely. Firstly note that

$$f_k(\mathcal{U}_k^{\text{obs}} | z_{\mathbb{S}_{\leq k}}) = 1 \iff \mathbf{A}_{\text{foc}}(Z_{\mathbb{S}_{\leq k}}^{\text{obs}}; \mathcal{S}_{k,\ell}) = \mathbf{A}_{\text{foc}}(z_{\mathbb{S}_{\leq k}}; \mathcal{S}_{k,\ell}) \quad \forall \ell \in [L_k].$$

Suppose the LHS of (16) is 1, then it's easy to see that $\mathbf{A}_{\text{foc}}(z_{\mathbb{S}_{\leq k}}; \mathcal{S}_{k,\ell}) = \mathbf{A}_{\text{foc}}(Z_{\mathbb{S}_{\leq k}}^{\text{obs}}; \mathcal{S}_{k,\ell})$ for all $\ell \in [L_k]$ by (10). Also, we can see $z_{\mathbb{S}_{\leq k}} \in \mathcal{Z}^{\text{obs}}$, which implies $g_k(\mathcal{Z}_k^{\text{obs}} | \mathcal{U}_k^{\text{obs}}, z_{\mathbb{S}_{\leq k}}) = 1$. Hence RHS is also 1. On the other hand, suppose the LHS of (16) is 0, then either for some $i \in \mathbb{S}_{\leq k} \setminus (\mathbf{A}_{\text{rand}}(Z_{\mathbb{S}_{\leq k}}^{\text{obs}}; \mathcal{S}_k) \setminus \mathbb{S}_{<k})$, $z_i \neq Z_i^{\text{obs}}$, or for some $i \in \mathbf{A}_{\text{foc}}(Z_{\mathbb{S}_{\leq k}}^{\text{obs}}; \mathcal{S}_k)$, $w_i(z_{\mathbb{S}_{\leq k}}) \notin \{w_k, w_{k+1}\}$. For the first case,

$$\{Z' \in \text{supp}(P) \cap \mathbb{S}_{\leq k} : Z'_{\mathbb{S}_{\leq k} \setminus (\mathcal{N}(\mathcal{U}_k) \setminus \mathbb{S}_{<k})} = z_{\mathbb{S}_{\leq k} \setminus (\mathcal{N}(\mathcal{U}_k) \setminus \mathbb{S}_{<k})}, w_i(Z'_{\mathbb{S}_{\leq k}}) \in \{w_k, w_{k+1}\}, \forall i \in \mathcal{U}_k\} \neq \mathcal{Z}^{\text{obs}},$$

because for any $z'_{\mathbb{S}_{\leq k}} \in \mathcal{Z}^{\text{obs}}$ we will have $z'_i = Z_i^{\text{obs}} \neq z_i$ for that particular i , so that $g_k(\mathcal{Z}_k^{\text{obs}} | \mathcal{U}_k^{\text{obs}}, z) = 0$. For the second case, there exists $\ell \in [L_k]$ and $i \in \mathbf{A}_{\text{foc}}(Z_{\mathbb{S}_{\leq k}}^{\text{obs}}; \mathcal{S}_{k,\ell})$ such that $w_i(z_{\mathbb{S}_{\leq k}}) \notin \{w_k, w_{k+1}\}$. But that means $\mathbf{A}_{\text{foc}}(z_{\mathbb{S}_{\leq k}}; \mathcal{S}_{k,\ell}) \neq \mathbf{A}_{\text{foc}}(Z_{\mathbb{S}_{\leq k}}^{\text{obs}}; \mathcal{S}_{k,\ell})$ so that $f_k(\mathcal{U}_k^{\text{obs}} | z_{\mathbb{S}_{\leq k}}) = 0$. As a result, (16) holds, and by Theorem 1 in Basse et al. (2019), for any $\alpha \in [0, 1]$,

$$\mathbb{P}\left(\text{pval}_k \leq \alpha \mid Z_{\mathbb{S}_{<k}}^{\text{obs}}, \mathcal{U}_k^{\text{obs}}, \tilde{H}_{0k}\right) \leq \alpha,$$

where the probability is taken with respect to the design conditional on realizations of $Z_{\mathbb{S}_{<k}}^{\text{obs}}$ and $\mathcal{U}_k^{\text{obs}}$ being the active focal units. This implies

$$\mathbb{P}\left(\text{pval}_k \leq \alpha \mid Z_{\mathbb{S}_{<k}}^{\text{obs}}; \tilde{H}_{0k}\right) \leq \alpha,$$

where the probability is taken with respect to the design conditional on realizations of $Z_{\mathbb{S}_{<k}}^{\text{obs}}$ solely.

2. p_k is valid for H_{0k} : This follows from a similar argument in [Caughey et al. \(2023\)](#) Theorem A1, by recognizing the two exposure levels w_k and w_{k+1} as “controlled” and “treated” separately as in the binary treatment setting with no interference. The p -value pval_k in (11) can be equivalently written as (ignoring conditioning and subscripts for brevity)

$$\text{pval}_k = \mathbb{P}_{w \sim r_{k,w}}\left(t(w, Y^{\text{obs}}; \mathcal{U}_k^{\text{obs}}) \geq t(w^{\text{obs}}, Y^{\text{obs}}; \mathcal{U}_k^{\text{obs}})\right),$$

where $w = (w_i)_{i \in \mathcal{U}_k^{\text{obs}}}$ is the vector of exposures for units in $\mathcal{U}_k^{\text{obs}}$, $\mathcal{U}_k^{\text{obs}} = \text{A}_{\text{foc}}(Z_{\mathbb{S}_{\leq k}}^{\text{obs}}; \mathbb{S}_k)$ the set of all active focal units almost surely, $w_i^{\text{obs}} = w_i(Z_{\mathbb{S}_{\leq k}}^{\text{obs}})$ the observed exposures, and

$$r_{k,w}(w = (w^i)_{i \in \mathcal{U}_k^{\text{obs}}}) = \sum_{z_{\mathbb{S}_{\leq k}}} \mathbb{1}\{w_i(z_{\mathbb{S}_{\leq k}}) = w^i, \forall i \in \mathcal{U}_k^{\text{obs}}\} r_k(z_{\mathbb{S}_{\leq k}}), \quad \forall (w^i)_{i \in \mathcal{U}_k^{\text{obs}}} \in \{w_k, w_{k+1}\}^{|\mathcal{U}_k^{\text{obs}}|},$$

is the distribution over exposures in $\mathcal{U}_k^{\text{obs}}$ induced by the randomization distribution r_k . Let $\tau_{k,i} := y_i(0, w_{k+1}) - y_i(0, w_k)$ as the true “treatment effect” of exposure w_{k+1} versus w_k . Suppose H_{0k} holds, then we have $\tau_{k,i} \leq 0$ for all i . Note that for all $i \in \mathcal{U}_k^{\text{obs}}$,

$$\begin{aligned} Y_i^{\text{obs}} - y_i(0, w_{k+1}) &= \mathbb{1}\{w_i^{\text{obs}} = w_k\}(-\tau_{k,i}) \geq 0 \\ Y_i^{\text{obs}} - y_i(0, w_k) &= \mathbb{1}\{w_i^{\text{obs}} = w_{k+1}\}(\tau_{k,i}) \leq 0. \end{aligned}$$

Since $Y_i^{\text{obs}} = y_i(0, w_i) + \mathbb{1}\{w_i = w_{k+1}\}(Y_i^{\text{obs}} - y_i(0, w_{k+1})) + \mathbb{1}\{w_i = w_k\}(Y_i^{\text{obs}} - y_i(0, w_k))$, by the definition of exposure monotonicity, $t(w, Y^{\text{obs}}; B_k) \geq t(w, (y_i(0, w_i))_i; B_k)$. Hence,

$$\begin{aligned} \text{pval}_k &= \mathbb{P}_{w \sim r_{k,w}}\left(t(w, Y^{\text{obs}}; \mathcal{U}_k^{\text{obs}}) \geq t(w^{\text{obs}}, Y^{\text{obs}}; \mathcal{U}_k^{\text{obs}})\right) \\ &\geq \mathbb{P}_{w \sim r_{k,w}}\left(t(w, (y_i(0, w_i))_i; \mathcal{U}_k^{\text{obs}}) \geq t(w^{\text{obs}}, Y^{\text{obs}}; \mathcal{U}_k^{\text{obs}})\right) =: \text{pval}_k^*. \end{aligned}$$

Under H_{0k} , pval_k^* stochastically dominates Uniform $(0, 1)$ following the same reasoning in step 1 with only a modification that we impute missing potential outcomes using both Y^{obs} and $(\tau_{k,i})_i$. Hence, for any $\alpha \in [0, 1]$,

$$\mathbb{P}\left(\text{pval}_k \leq \alpha \mid Z_{\mathbb{S}_{<k}}^{\text{obs}}; H_{0k}\right) \leq \mathbb{P}\left(\text{pval}_k^* \leq \alpha \mid Z_{\mathbb{S}_{<k}}^{\text{obs}}; H_{0k}\right) \leq \alpha.$$

3. Stochastically larger than Uniform: Recall in Algorithm 2 from each step $k = 1, \dots, K - 1$, we apply Algorithm 1' with module set \mathbb{S}_k , observed treatment Z^{obs} , conditional set $\mathbb{S}_{<k}$, and get p -value pval_k . Essentially we only input the observed treatment $Z_{\mathbb{S}_{\leq k}}^{\text{obs}}$ on $\mathbb{S}_{\leq k}$. As a result, pval_k can be written as a function of $\text{pval}_k(Z_{\mathbb{S}_{\leq k}}^{\text{obs}}) = \text{pval}_k(Z_{\mathbb{S}_1}^{\text{obs}}, \dots, Z_{\mathbb{S}_k}^{\text{obs}})$. The result follows from Lemma 1 by taking $Q_k = Z_{\mathbb{S}_k}^{\text{obs}}$. \square

A.3 Proof of Theorem 2

Proof of Theorem 2. The fact that each pval_k is valid under H_{0k} , that is,

$$\mathbb{P}_{Z_{V_k}^{\text{obs}} \sim P_k(\cdot)}\left(\text{pval}_k \leq \alpha_k \mid \{\mathcal{C}_j^k\}_{j \in J_k}, (Z_i^{\text{obs}})_{i \in V_{<k}}, H_{0k}\right) \leq \alpha_k, \quad (17)$$

for all k and $\alpha_k \in [0, 1]$, follows directly from Proposition 1 in Appendix D by taking $P(\cdot)$ as $P(\cdot \mid Z_{\cup_{k' <k} V_{k'}}^{\text{obs}})$.

In addition, the k -th biclique decomposition $\{\mathcal{C}_j^k\}_{j \in J_k}$ is computed using the $P_k(Z_{V_k}) = P(Z_{V_k} \mid Z_{V_{<k}}^{\text{obs}})$ (and the partition of the network, which we considered as fixed), so that it is a function of $Z_{V_{<k}}^{\text{obs}}$. Given the k -th biclique decomposition $\{\mathcal{C}_j^k\}_{j \in J_k}$, the biclique test defines a selection mechanism s_k that maps any Z_{V_k} into the unique biclique $\mathcal{C} = (\mathcal{U}, \mathcal{Z}) \in \{\mathcal{C}_j^k\}_{j \in J_k}$ such that $Z_{V_k} \in \mathcal{Z}$. s_k maps the observed $Z_{V_k}^{\text{obs}}$ into the $\mathcal{C}^{k,\text{obs}} = (\mathcal{U}^{k,\text{obs}}, \mathcal{Z}^{k,\text{obs}})$ that is used in the randomization test, so that $\mathcal{C}^{k,\text{obs}}$ is a function of $Z_{V_k}^{\text{obs}}$. Moreover, the k -th randomization distribution (Line 3 of Algorithm 4) is given by

$$r_k(Z_{V_k}) \propto \mathbb{1}\{Z_{V_k} \in \mathcal{Z}^{k,\text{obs}}\} P_k(Z_{V_k}) = \mathbb{1}\{Z_{V_k} \in \mathcal{Z}^{k,\text{obs}}(Z_{V_k}^{\text{obs}})\} P(\cdot \mid Z_{V_{<k}}^{\text{obs}}),$$

which shows that $r_k(\cdot)$ is a function of $Z_{V_{<k}}^{\text{obs}}$. Altogether, the k -th p -value pval_k is a function of

$Z_{V_{\leq k}}^{\text{obs}}$. Taking $Q_k = Z_{V_k}^{\text{obs}}$ in Lemma 1, from (17), we conclude that $(\text{pval}_k)_k$ are stochastically larger than uniform, which finishes the proof. \square

B Combination of p -values

There are many other ways one can combine the p -values resulting from each sub-hypothesis H_{0k} apart from Fisher’s rule. A general condition is given by the lemma below.

Lemma 2 (Rosenbaum (2011), Lemma 1). *If $f : [0, 1]^K \rightarrow \mathbb{R}$ is monotone decreasing in each of the K coordinates and (P_1, \dots, P_K) is stochastically larger than uniform, then $f(P_1, \dots, P_K) \lesssim^{\text{1st}} f(P_1^*, \dots, P_K^*)$ where $P_k^* \stackrel{iid}{\sim} U(0, 1)$ and \lesssim^{1st} denotes first-order stochastic dominance.*

Therefore one can compare the observed value of $f(P_1, \dots, P_K)$ with quantiles of $f(P_1^*, \dots, P_K^*)$ for $P_k^* \stackrel{iid}{\sim} U(0, 1)$, which can be calculated exactly or approximated by Monte-Carlo. Some examples include Stouffer’s weighted z -score (Stouffer et al., 1949) and the Cauchy combination rule (Liu and Xie, 2019). Existing theory has pointed out that no single method of combining independent tests of significance is optimal in general (Birnbaum, 1954).

In our context, we prefer Fisher’s combination for the behavior of its log-transformation when p -values are close to 0 or 1 (see Table 3). When the null is violated at some of the sub-hypothesis H_{0k} , and the signal strength is quite strong so that $p_k \rightarrow 0$ and $p_{k'} \rightarrow 1$ for all $k' \neq k$ (or the other way), where p_k is the p -value for testing H_{0k} , both Stouffer and Cauchy combination involve expression of $+\infty - \infty$, making the combined p -value unstable. This is the case in DGP2 of Section 6.3 when $\tau \neq 0$. In that setup, p_1 provides an opposite signal of the monotone null compared to p_2 and p_3 , as shown in Figure 9 where we plot the rejections of each individual hypothesis and the combined rejection of the monotone hypothesis. Here we truncate each p -value to be within $[\epsilon, 1 - \epsilon]$ with $\epsilon = 10^{-4}$ before the CDF transformation $\Phi^{-1}(\cdot)$, and the truncation binds when $|\tau|$ is large. When using the number of active focal units to be the weights, the combination makes p_1 overly dominant because there are more

active focal units for testing H_{01} (as can be seen in Figure 7), so that the Stouffer’s method becomes powerless in rejecting $\tau > 0$. The problem remains for other weighting schemes.

	$p_k \rightarrow 0$	$p_{k'} \rightarrow 1$	Combination of p_k and $p_{k'}$
Fisher	$\log p_k \rightarrow -\infty$	$\log p_{k'} \rightarrow 0$	FCT $\rightarrow -\infty$
Stouffer	$\Phi^{-1}(p_k) \rightarrow -\infty$	$\Phi^{-1}(p_{k'}) \rightarrow +\infty$	Stouffer $\rightarrow +\infty - \infty$
Cauchy	$\tan((0.5 - p_k)\pi) \rightarrow -\infty$	$\tan((0.5 - p_{k'})\pi) \rightarrow +\infty$	CCT $\rightarrow +\infty - \infty$

Table 3: Behavior of transformed p -values under extreme values for Fisher, Stouffer and Cauchy combination rule.

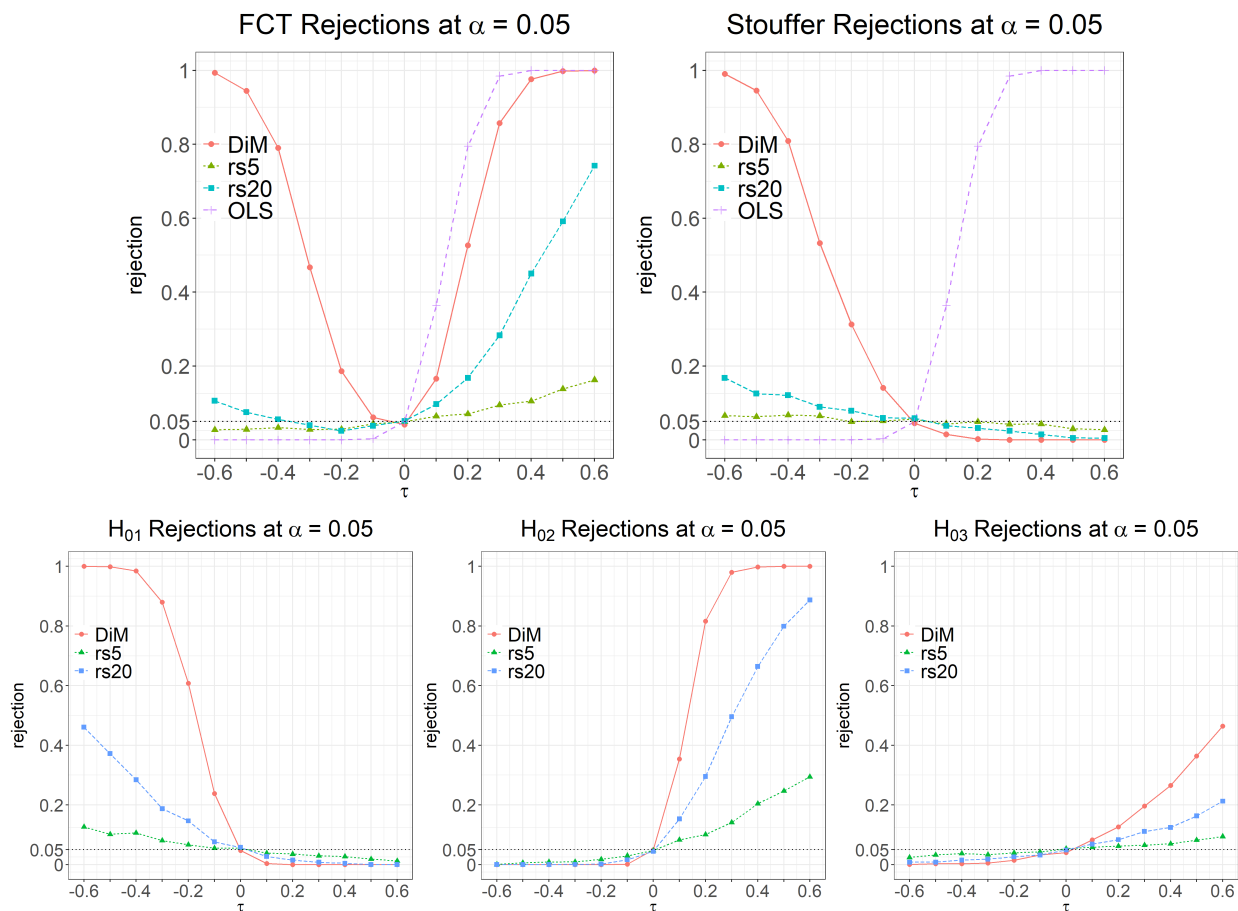


Figure 9: Rejection of overall monotone hypothesis and individual hypotheses under DGP2.

Another approach would be to not split the network at all, test each individual null hypothesis H_{0k} on the entire network, and combine the resulting p -values using Bonferroni’s method. Although Bonferroni’s rule usually leads to power loss, this approach may be competitive in settings where we suspect that the violation of monotonicity is mainly due

to one particular contrast, e.g., having “1 neighbor treated” vs. “0 neighbors treated”, or testing all but a few of the sub-hypotheses is difficult due to, for example, lack of eligible or active focal units after splitting the network.

One final remark is that the default Fisher’s combination puts equal weights on each of the p -values. This is plausible without any prior knowledge. Some interesting exceptions may exist when, for example, we suspect “diminishing returns” in the spillover effect, or the violation of monotonicity is mainly due to one particular contrast of the exposures. In such cases, it may be better to put more weights on some hypotheses over others as that could lead to more power compared to the default Fisher’s combination rule. We can also weight the p -values by the number of active focal units used in the test, as we do for the Stouffer’s combination in Section 6.2.

C More on the module-based Algorithm

C.1 Further extensions of Algorithm 1’

Exposures beyond neighbors For $w_i(z)$ that depends on the treatments of units beyond \mathcal{N}_i , we can analogously define $E_{\text{rand}}(\mathcal{S}_\ell)$ to include units whose treatment status determines $w_i(z)$ for all $i \in E_{\text{foc}}(\mathcal{S}_\ell)$, i.e., $E_{\text{rand}}(\mathcal{S}_\ell)$ is a set of units such that for all $i \in E_{\text{foc}}(\mathcal{S}_\ell)$, $y_i(z) = y_i(z')$ for all $z, z' \in \{0, 1\}^N$ such that $z_{E_{\text{rand}}(\mathcal{S}_\ell) \cup \{i\}} = z'_{E_{\text{rand}}(\mathcal{S}_\ell) \cup \{i\}}$. The remaining definitions of modules, module sets, active focal/randomization units and procedures in Algorithm 1’ are kept unchanged.

Designs beyond non-uniform Bernoulli The assumption of Bernoulli design is used to calculate the conditional randomization distribution over active focal units in Lines 4-5 and Lines 8-12 in Algorithm 1, or Lines 2-4 in Algorithm 1’. In particular, when sampling from the randomization distribution in Lines 8-12 of Algorithm 1 or Lines 2-4 in Algorithm 1’, we rely on the assumption that treatments across $E_{\text{rand}}(\mathcal{S}_\ell)$ are independent, which follows from

the Bernoulli design. We can relax the Bernoulli design to a “clustered” one where the design has a factorization $P(Z) = P_c(Z_{S^c}) \prod_{\ell} P_{\ell}(Z_{S_{\ell}})$ by appropriately choosing the modules, so that treatments across $(S_{\ell})_{\ell}$ are independent of each other, while not affecting the validity of the randomization test. Under the clustered design, the randomization distribution for \tilde{Z}_{ℓ} can be calculated exactly or approximated to any precision using the same procedure as in Section 4.2.1. Note, however, that such a calculation is tractable only when the size of each cluster, $|S_{\ell}|$, is moderate. Otherwise, calculating the randomization distribution will be computationally challenging. In such cases, it’s better to use the clique-based approach in Section 5, in which the cluster naturally provides a partition of the whole network.

C.2 Implementation details in the Medellín example

In the Medellín example in Section 6 and 7, there are far more units that will always stay in control (the $37,055 - 967 = 36,088$ non-hotspots) compared to those with positive treatment probabilities (the 967 hotspots). Using this fact, Algorithm 1 and 2 can be implemented with great simplification. Firstly, the edge set E can be defined as $\{(i, j) \in [N]^2 : d(i, j) \leq r, \text{ and at least one of } i, j \text{ is hotspot}\}$. Secondly, in constructing the module sets, we can choose all $E_{\text{foc}}(\mathcal{S})$ to be non-hotspots and all $E_{\text{rand}}(\mathcal{S})$ to be hotspots only. The requirement $E_{\text{rand}}(\mathcal{S}_{\ell}) \cap E_{\text{rand}}(\mathcal{S}_{\ell'}) = \emptyset$ is then equivalent to requiring that eligible focal units in different modules do not share the same hotspot within a distance r . Constructing uniform modules is also straightforward in regions where hotspots are relatively rare compared to non-hotspots, such as the outskirts of the city as shown in Figure 5, in which case all the nearby non-hotspots will be in the same $E_{\text{foc}}(\mathcal{S})$.

Another practical consideration of the algorithm is how to construct modules to have meaningful randomizations. The randomization in Lines 10-11 of Algorithm 1 essentially draws exposures from $\{w_k, w_{k+1}\}$ on $A_{\text{foc}}(Z^{\text{obs}}; \mathcal{S}_{\ell})$. Ideally, the induced distribution on exposures of $A_{\text{foc}}(Z^{\text{obs}}; \mathcal{S}_{\ell})$ should not be degenerate, i.e., $p_{\ell} \in (0, 1)$ for all ℓ . We could enforce this condition in the construction of module sets by selecting each $E_{\text{foc}}(\mathcal{S}_{\ell})$ from the

set $\mathfrak{S}_k := \{i : w_i^{\text{all}} \geq w_{k+1}, w_i^{\text{none}} \leq w_k\}$, where w_i^{all} and w_i^{none} are the exposures of i when all and none of i 's neighboring hotspots are treated, with the exception that units j with $p_j = 0$ ($p_j = 1$) always stay in control (treated). Then by a continuity argument we know $p_\ell \in (0, 1)$.

The histogram of the number of eligible and active focal units when running the algorithm on multiple independent constructions of module sets is presented in Figure 7 in the main text. Many eligible focal units are utilized in the randomization test by being active. Notably, although not displayed, none of the active focal units has a degenerate randomization distribution due to the construction above.

D A review of the biclique test

Denote $\mathbb{U} = [N]$ and $\mathbb{Z} = \{z \in \{0, 1\}^N : P(z) > 0\}$. As said in the main text, the key idea behind the biclique test of Puelz et al. (2022) is to translate the conditioning step in the construction of a conditional randomization test into a biclique decomposition of an appropriate graphical representation of the null hypothesis \tilde{H}_{0k} . To be specific, we need the following definitions.

Definition 5 (Null exposure graph and bicliques.). The null exposure graph with respect to \tilde{H}_{0k} is a bipartite graph $\mathcal{G}_k^{\text{ne}} = (V_k^{\text{ne}}, E_k^{\text{ne}})$ such that $V_k^{\text{ne}} = \mathbb{U} \cup \mathbb{Z}$, and an edge between $(i, z) \in \mathbb{U} \times \mathbb{Z}$ exists in E_k^{ne} if and only if $z_i = 0$ and $w_i(z) \in \{w_k, w_{k+1}\}$. A biclique of a null exposure graph $\mathcal{G}_k^{\text{ne}} = (V_k^{\text{ne}}, E_k^{\text{ne}})$ is a subgraph $\mathcal{C} = (\mathcal{U}, \mathcal{Z})$, where $\mathcal{U} \subseteq \mathbb{U}$ and $\mathcal{Z} \subseteq \mathbb{Z}$, such that each unit $i \in \mathcal{U}$ is connected to all assignments in \mathcal{Z} , i.e., $\mathcal{U} \times \mathcal{Z} \subseteq E_k^{\text{ne}}$.

The null exposure graph encodes the ‘‘imputability pattern’’ under the null hypothesis. That is, if z and z' are both connected to a unit i in the null exposure graph, then $Y_i(z) = Y_i(z')$ under the null hypothesis. As a result, the potential outcomes involved in \tilde{H}_{0k} for all units in a biclique can be imputed under the null hypothesis by their observed outcomes for *all* treatment assignments in the biclique if the observed Z^{obs} is also in the biclique.

Algorithm 4 (Puelz et al., 2022) Biclique test for $\tilde{H}_{0k} : y_i(0, \mathbf{w}_k) = y_i(0, \mathbf{w}_{k+1})$

Require: Observed treatment Z^{obs} ; design $P(\cdot)$ (Input).

Output: Finite-sample valid p -value for \tilde{H}_{0k} .

- 1: Construct the null exposure graph $\mathcal{G}_k^{\text{ne}}$ using $\mathbb{U} = [N]$ and \mathbb{Z} .
- 2: Decompose $\mathcal{G}_k^{\text{ne}}$ to obtain $\{\mathcal{C}_j\}_{j \in J}$, and find the unique biclique $\mathcal{C}^{\text{obs}} = (\mathcal{U}^{\text{obs}}, \mathcal{Z}^{\text{obs}}) \in \{\mathcal{C}_j\}_{j \in J}$ such that $Z^{\text{obs}} \in \mathcal{Z}^{\text{obs}}$.
- 3: Define the randomization distribution $r(Z) \propto \mathbb{1}\{Z \in \mathcal{Z}^{\text{obs}}\} \cdot P(Z)$.
- 4: Calculate the p -value as follows:

$$\text{pval}(Z^{\text{obs}}, Y^{\text{obs}}; \mathcal{C}^{\text{obs}}) = \mathbb{E}_{Z \sim r(\cdot)} \left[\mathbb{1}\{t(Z, Y^{\text{obs}}; \mathcal{C}^{\text{obs}}) > t(Z^{\text{obs}}, Y^{\text{obs}}; \mathcal{C}^{\text{obs}})\} \right]. \quad (18)$$

In light of these imputability results, the biclique test of Puelz et al. (2022) proceeds in three main steps presented in Algorithm 4. First, they build the null exposure graph that uniquely corresponds to the null hypothesis being tested and the particular treatment exposure function $w_i(\cdot)$ under the design $P(\cdot)$. Next, they compute a biclique decomposition of the null exposure graph, a collection of bicliques $\{\mathcal{C}_j\}_{j \in J}$ with $\mathcal{C}_j = (\mathcal{U}_j, \mathcal{Z}_j)$, such that $\{\mathcal{Z}_j\}_{j \in J}$ forms a partition⁶ of \mathbb{Z} . Such decomposition can be implemented efficiently using several existing graph algorithms⁷. Finally, a conditional randomization test is executed within the biclique $\mathcal{C}^{\text{obs}} = (\mathcal{U}^{\text{obs}}, \mathcal{Z}^{\text{obs}})$, one of the \mathcal{C}_j 's such that $Z^{\text{obs}} \in \mathcal{Z}^{\text{obs}}$, which reduces to a weighted sampling over the treatment assignments in \mathcal{Z}^{obs} using $P(z)$ as the weights.

Theorem 2 of Puelz et al. (2022) establishes the finite-sample validity of the test for \tilde{H}_{0k} . Moreover, using a similar reasoning as in Theorem 1 of our paper, when using an exposure-monotone test statistic in the order $(\mathbf{w}_k, \mathbf{w}_{k+1})$, the biclique test is also valid for testing the single monotone hypothesis $H_{0k} : y_i(0, \mathbf{w}_k) \geq y_i(0, \mathbf{w}_{k+1}) \forall i$.

Proposition 1. *Consider applying Algorithm 4 to test \tilde{H}_{0k} . When an exposure-monotone test statistic in the order $(\mathbf{w}_k, \mathbf{w}_{k+1})$ is applied in Line 4, the resulting p -value in (18) is also*

⁶That is, $\mathcal{Z}_i \cap \mathcal{Z}_j = \emptyset$ for $i \neq j$, and $\bigcup_{j \in J} \mathcal{Z}_j = \mathbb{Z}$.

⁷For example, the “binary inclusion-maximal biclustering” (Bimax) algorithm as used in Puelz et al. (2022), and the “imBEA” algorithm in Zhang et al. (2014).

valid under H_{0k} in Equation (4). That is, for any $\alpha \in [0, 1]$,

$$\mathbb{P}_{Z^{\text{obs}} \sim P(\cdot)} \left(\text{pval}(Z^{\text{obs}}, Y^{\text{obs}}; \mathcal{C}^{\text{obs}}) \leq \alpha \mid \{\mathcal{C}_j\}_{j \in J}, H_{0k} \right) \leq \alpha.$$

E Assignment of clusters to hypotheses

In this section we present a way to partition the network using an algorithm in the community detection literature, and subsequently find matches between hypotheses to test and the partitions leveraging the clique-based test in Section 5. We also present power simulation results under the setup in Section 6.

E.1 Network partitioning

As discussed in the main text, heuristically we would want the partition of the network to maximize connections between nodes within each sub-network, while minimizing the connections between nodes across different sub-networks. The Leiden algorithm (Traag et al., 2019) is considered a computationally efficient algorithm to detect such sub-networks (or “communities”, “clusters”) with some theoretical guarantee of the well-connectedness of the resulting sub-networks. When applying the algorithm iteratively, it is also guaranteed to converge to a partition in which all subsets of all sub-networks are locally optimal. The algorithm is widely adopted in various domains such as genetics (Heumos et al., 2023) and social science (Logan et al., 2023).

To use the Leiden algorithm there are three tuning parameters to specify: “resolution”, “beta”, and the number of iterations. Higher resolutions lead to more and smaller communities, while lower resolutions lead to fewer and larger communities, and “beta” affects the randomness in the algorithm. In the Medellín network, we specify the number of iterations to be 200, as we observed that it’s enough for the algorithm to stabilize. For some values of resolution and beta, the average number of communities detected across 5,000 repetitions of the algorithm are presented in Table 4. From the results, in the subsequent analysis we

choose “resolution” in $\{10^{-3}, 10^{-4}\}$ and “beta” in $\{10^{-1}, 10^{-2}, 10^{-3}\}$ to avoid too many small communities.

Resolution	Beta	# of communities detected
10^{-2}	10^{-1}	1841.00
10^{-3}	10^{-1}	107.50
10^{-4}	10^{-1}	54.77
10^{-2}	10^{-2}	1826.92
10^{-3}	10^{-2}	107.02
10^{-4}	10^{-2}	54.79
10^{-2}	10^{-3}	1824.32
10^{-3}	10^{-3}	105.47
10^{-4}	10^{-3}	54.70

Table 4: Leiden algorithm: resolution and beta and number of communities, average across 5,000 repetitions of the algorithm

E.2 Assigning communities to hypotheses

Given the detected communities, or sub-networks $\mathcal{G}_c = (V_c, E_c)$ with $c \in [C]$, we need to decide which sub-networks are used to test which of the $K - 1$ hypotheses H_{0k} . We will formulate such a decision problem into an optimization problem that can be solved efficiently.

Denote $S_c = |V_c|$ the size of the community c , $\text{NE}_{c,k}$ the matrix representation of the null exposure graph built within \mathcal{G}_c under hypothesis H_{0k} , with $\dim(\text{NE}_{c,k}) = S_c \times N_{\text{rand}}$ where N_{rand} is the number of randomizations drawn from $P_k(\cdot)$, and the (i, j) -th entry $\text{NE}_{c,k}[i, j] = 1$ if and only if the i -th node is connected to the j -th randomization. Let $M_{c,k}$ be a measurement of the “informativeness” of $\text{NE}_{c,k}$, such as

- density of $\text{NE}_{c,k}$: $M_{c,k} = \sum_{i,j} \text{NE}_{c,k}[i, j] / (S_c \cdot N_{\text{rand}})$;
- average standard deviations across rows: $M_{c,k} = \sum_i \text{sd}(\text{NE}_{c,k}[i, :]) / S_c$;
- average standard deviations across columns: $M_{c,k} = \sum_j \text{sd}(\text{NE}_{c,k}[:, j]) / N_{\text{rand}}$.

Denote $A_{c,k}$ be the indicator of community c being assigned to test H_{0k} . We propose to solve

the assignment $A = (A_{c,k})$ through the following integer programming problem:

$$\begin{aligned}
& \max_A \min_{k \in [K-1]} \sum_{c \in [C]} A_{c,k} M_{c,k} S_c \\
& \text{s.t.} \quad \sum_{k \in [K-1]} A_{c,k} = 1, \quad \forall c \\
& \quad \quad \sum_{c \in [C]} A_{c,k} \geq 1, \quad \forall k \\
& \quad \quad A_{c,k} \in \{0, 1\}, \quad \forall c, k,
\end{aligned} \tag{19}$$

or equivalently the following MILP:

$$\begin{aligned}
& \max_{A, t} t \\
& \text{s.t.} \quad \sum_{c \in [C]} A_{c,k} M_{c,k} S_c \geq t, \quad \forall k \\
& \quad \quad \sum_{k \in [K-1]} A_{c,k} = 1, \quad \forall c \\
& \quad \quad \sum_{c \in [C]} A_{c,k} \geq 1, \quad \forall k \\
& \quad \quad A_{c,k} \in \{0, 1\}, \quad \forall c, k.
\end{aligned} \tag{20}$$

Without prior information, we treat each hypothesis equally by maximizing the minimum of a weighted score of the informativeness in testing hypothesis k . For example, when $M_{c,k}$ is the density of the null exposure graph, $M_{c,k} S_c$ calculates the sum of the NE graph densities for testing H_{0k} weighted by the size S_c , or equivalently the number of connections in the NE graphs that are used to test H_{0k} , modulo N_{rand} . The constraint $\sum_k A_{c,k} = 1$ imposes that each community c is used to test exactly one H_{0k} , and the constraint $\sum_c A_{c,k} \geq 1$ imposes that there should be at least one community assigned to test H_{0k} . Both (19) and (20) can be solved efficiently using optimization packages. An approximate solution is sufficient for our purpose.

Figure 10, 11 and 12 display some realizations of the network splitting and the focal units from solving the above optimization problem. As a baseline, we also present a naive

way to split the network in Figure 13 where the two break points in the x -coordinate are the 60% and 70% quantiles of the x -coordinates of the 967 hotspots, and the break point in the y -coordinate is the median of the y -coordinates of the 967 hotspots. Generally for all realizations there are fewer focal units for H_{02} and H_{03} .

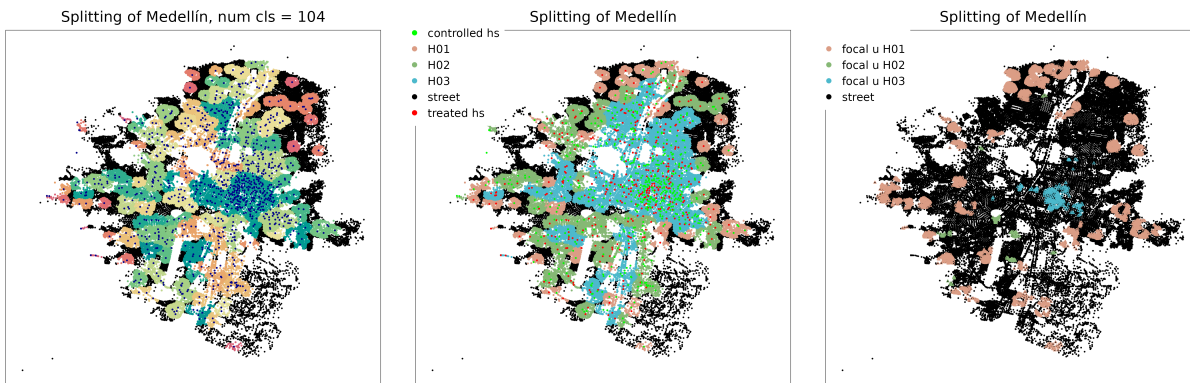


Figure 10: Leiden Splitting $(Res, Beta) = (10^{-3}, 10^{-1})$ results from one realization.

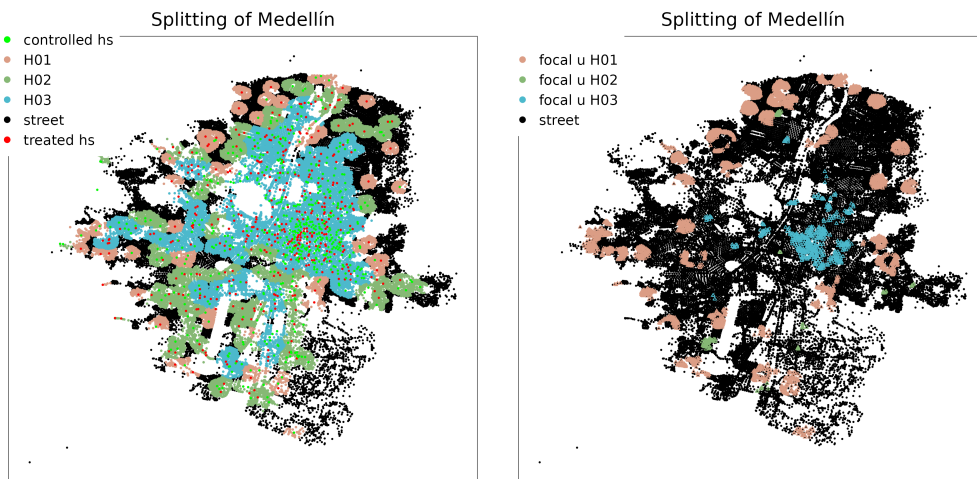


Figure 11: Leiden Splitting $(Res, Beta) = (10^{-3}, 10^{-1})$ results from another realization.

E.3 Power simulation

We use the DGP1 outcome model in Section 6.2, and 10,000 randomizations in constructing the bicliques. The results are in Figure 14 for Leiden algorithm $(Res, Beta) = (10^{-3}, 10^{-1})$

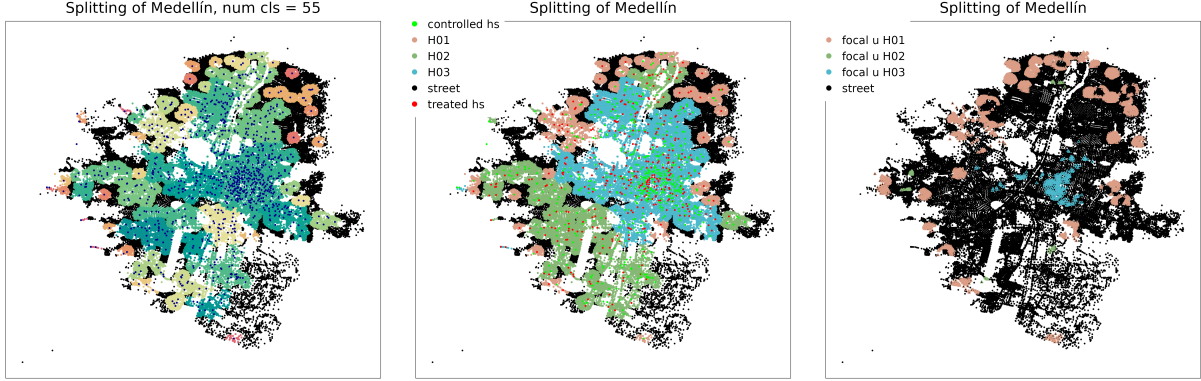


Figure 12: Leiden Splitting (Res, Beta) = $(10^{-4}, 10^{-1})$ results from one realization.

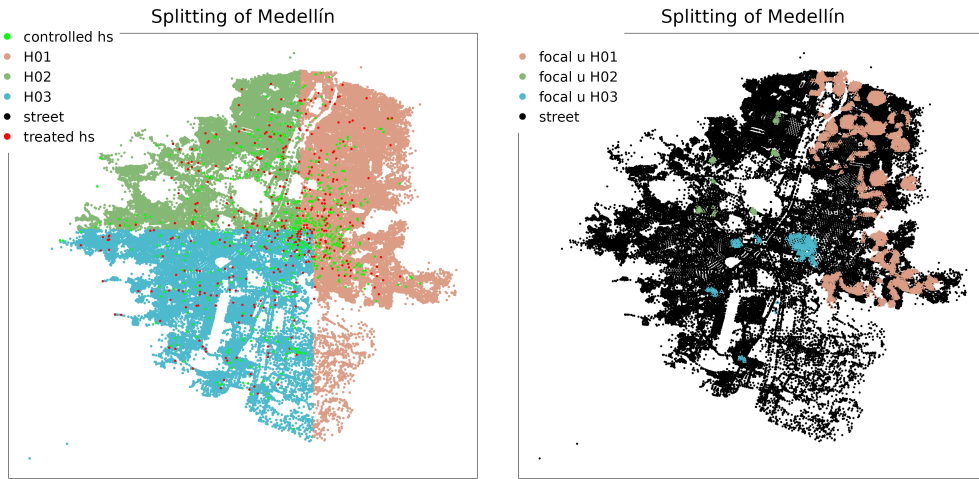


Figure 13: Naive splitting results.

and Table 5 for other parameters where we only present the power at $\tau \in \{-0.5, 0, 0.2, 0.5, 1\}$ with difference-in-means as the test statistic and p -values combined by Fisher's rule.

Method	$\tau = -0.5$	$\tau = 0$	$\tau = 0.2$	$\tau = 0.5$	$\tau = 1$
Leiden $(10^{-3}, 10^{-1})$	0.31	4.19	32.74	92.16	99.12
Leiden $(10^{-4}, 10^{-2})$	0.10	4.14	30.56	88.45	97.95
Leiden $(10^{-3}, 10^{-3})$	0.21	3.82	31.21	91.87	98.72
Leiden $(10^{-4}, 10^{-1})$	0.42	3.38	29.96	89.22	97.65
Leiden $(10^{-3}, 10^{-2})$	0.16	3.98	30.54	91.39	98.53
Leiden $(10^{-4}, 10^{-3})$	0.43	3.91	29.89	90.06	98.00
Naive splitting	0.30	3.81	22.88	77.49	96.71
Module-based test	0.00	5.15	62.25	100.00	100.00

Table 5: Simulation results for different splitting configurations under DGP1 in Section 6.2. All tests are conducted at the 5% level and the reported values are rejection probabilities (in %).

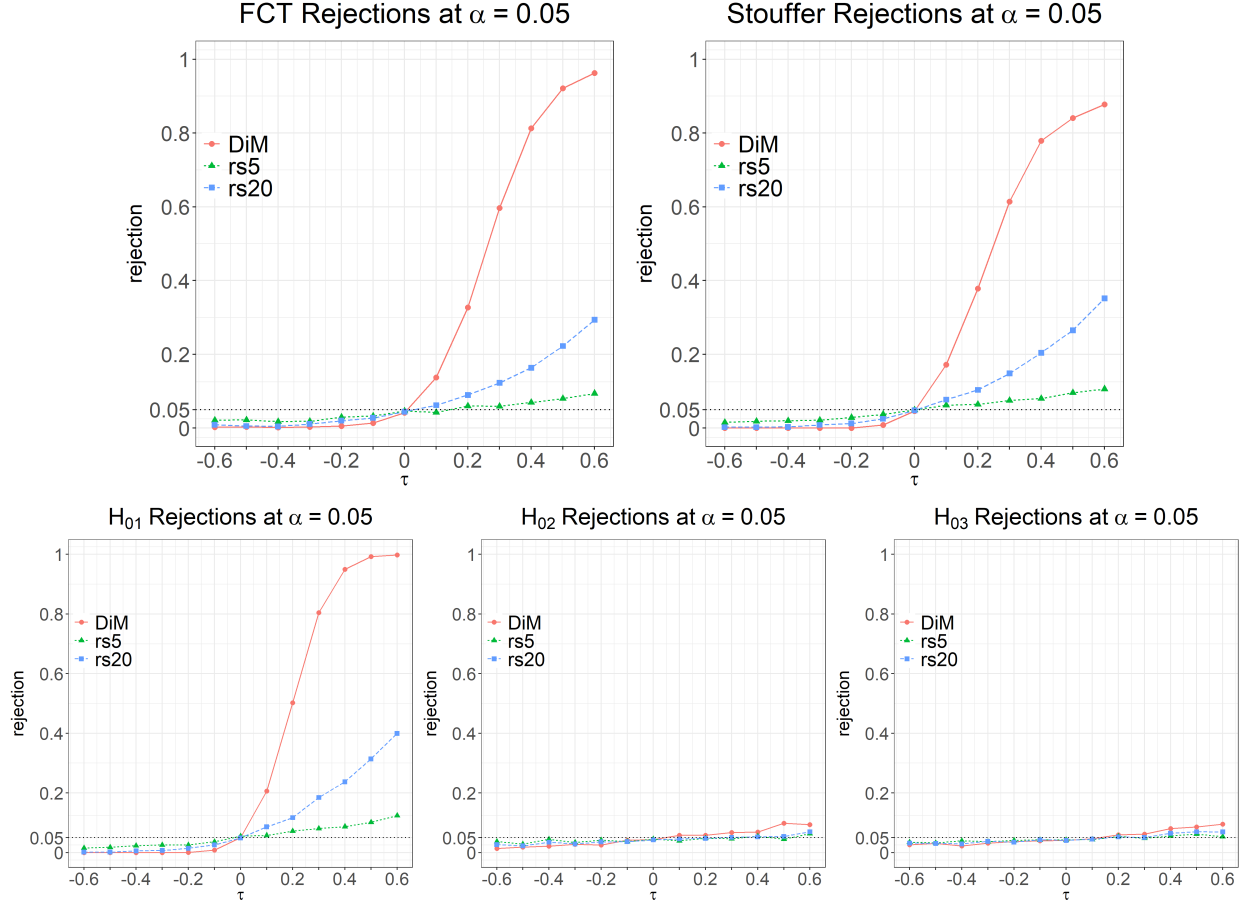


Figure 14: Leiden Splitting $(Res, Beta) = (10^{-3}, 10^{-1})$. Rejection of overall monotone hypothesis and individual hypotheses under DGP1 in Section 6.2

In general, there's little difference in power for different Leiden algorithm parameters. All of them are better than the naive way of splitting. Due to the lack of focal units, tests for H_{02} and H_{03} are of low power, making the clique-based test less powerful compared to the module-based test (Algorithm 2 of the main text).

F More Empirical Results

F.1 Justification of grouping exposure levels

In this section, we provide some empirical justification for the assumption that the (controlled) potential outcomes of a street are the same for all exposure levels of at least three. Specifically, we test the null hypothesis

$$H_0^{[\geq 3]} : y_i(0, w) = y_i(0, w'), \quad \forall w, w' \geq 3, \forall i, \quad (21)$$

where the exposure function is the number of treated neighbors within 225 meters as in the main text. Under the null hypothesis (21), consider the p -value from the following randomization test

$$\begin{aligned} \text{pval}(Z^{\text{obs}}) &= \mathbb{P}_{Z \sim P(\cdot)}(t(Z, Y^{\text{obs}}) \geq t(Z^{\text{obs}}, Y^{\text{obs}})), \\ t(Z, Y) &= \text{AIC}(\text{model 1}(Z, Y)) - \text{AIC}(\text{model 2}(Z, Y)), \end{aligned} \quad (22)$$

where $P(\cdot)$ is the design, and the test statistic is the difference in Akaike Information Criteria (AIC) between the OLS fits of the following two saturated linear models with grouping threshold 3 (model 1) and 10 (model 2)⁸, both fitted on non-hotspot streets only so that $Z_i = 0$ for all $Z \sim P(\cdot)$:

$$\begin{aligned} \text{model 1}(Z, Y) : \quad Y_i &= \sum_{k=0}^2 \theta_k \mathbb{1}\{w_i(Z) = k\} + \theta_3 \mathbb{1}\{w_i(Z) \geq 3\} + \varepsilon_i, \\ \text{model 2}(Z, Y) : \quad Y_i &= \sum_{k=0}^9 \theta_k \mathbb{1}\{w_i(Z) = k\} + \theta_{10} \mathbb{1}\{w_i(Z) \geq 10\} + \varepsilon_i. \end{aligned} \quad (23)$$

Under the null $H_0^{[\geq 3]}$, the two models are indistinguishable, so $t(Z^{\text{obs}}, Y^{\text{obs}})$ is expected not to lie in the tails of the randomization distribution — the distribution of $t(Z, Y^{\text{obs}})$ induced by $Z \sim P(\cdot)$. When $H_0^{[\geq 3]}$ does not hold, however, model 2 is expected to fit the outcome better, so $t(Z^{\text{obs}}, Y^{\text{obs}})$ is expected to lie in the right tail of the randomization distribution. The randomization distributions and the p -values for the six types of outcomes considered in the main text is presented in Figure 15. We observe that for all outcomes, we fail to reject $H_0^{[\geq 3]}$,

⁸From Figure 5 of the main text, a threshold of 10 is sufficient as there are few units with degree at least 10.

supporting our decision to group exposure levels beyond 3 into a single category. One final

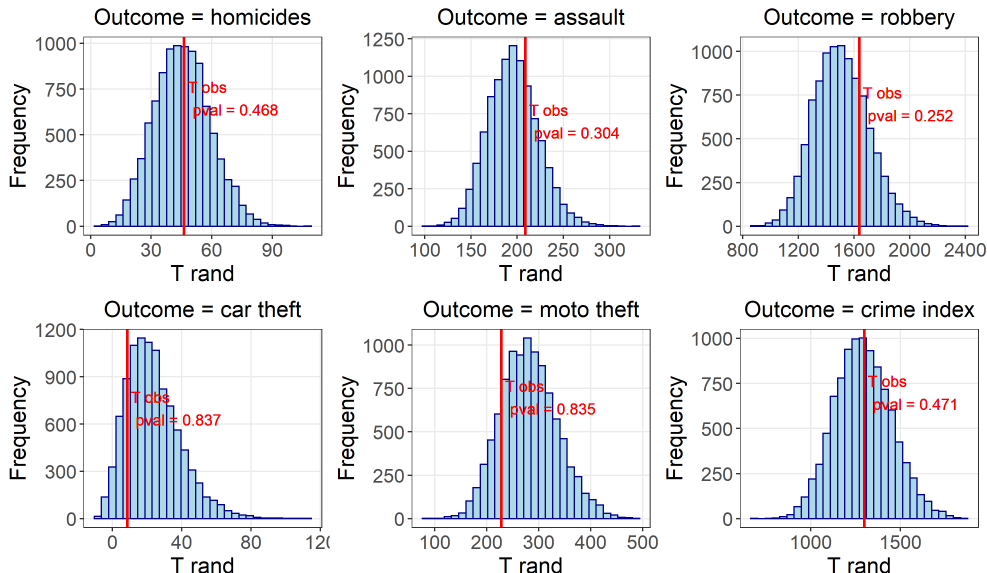


Figure 15: Randomization distributions and p -values for testing (21).

remark is that, instead of the AIC, one can use other (penalized) goodness-of-fit statistics, such as the difference in mean-squared errors or Bayesian Information Criteria, potentially applied to models other than the linear ones considered here.

F.2 Confounding factors

In the Medellín setting, when a street has many hotspots around, it is expected that the crime level in that street is high because of the proximity to the disturbing streets. Indeed, the two boxplots in Figure 16 shows that under Z^{obs} , degrees differ systematically across treatment and exposure levels. This suggests that d_i may act as a confounder when regressing the outcome on treatment and exposure, even if one fully saturates at exposure as in (23), and motivates the DGP3 in Section 6.2 of the main text. We also note that many such confounders may exist in real-life settings, making standard inference methods unreliable.

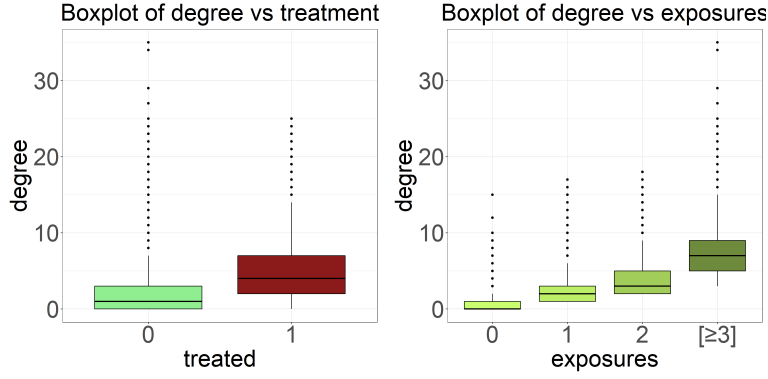


Figure 16: Boxplots of degree vs treatment and exposure levels

F.3 More results on the monotone hypothesis

Results from different constructions of module sets. Figure 17 shows the histograms of the p -values resulting from 2,000 independent constructions of module sets for the crime index outcome. Table 6 presents twice the median of the 2,000 p -values for all the outcomes. Both are for the beneficial spillover hypothesis (14). We reject (14) at 5% level for all outcomes using the rank-sum test statistic.

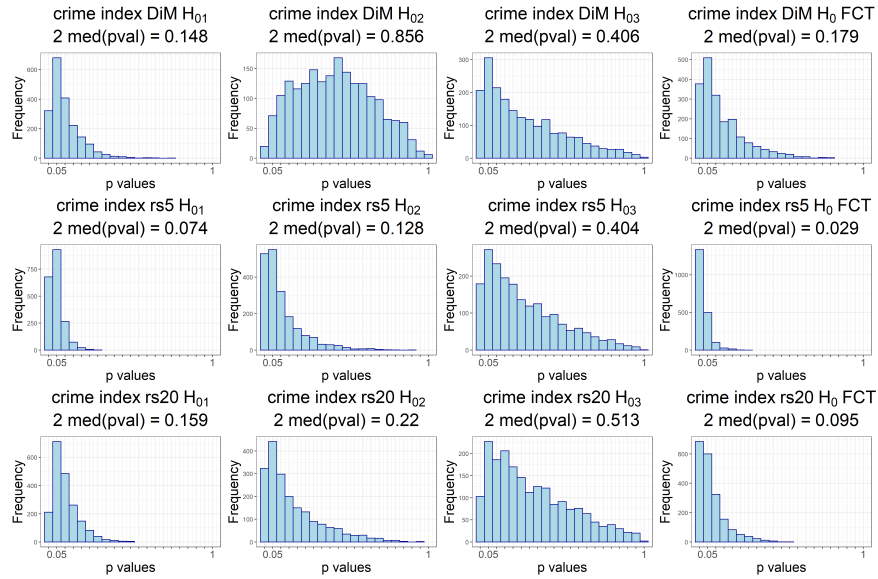


Figure 17: Histograms of p -values for crime index across the 2,000 constructions.

Hypothesis	test stat	homicides	assault	robbery	car theft	moto theft	crime index
H_{01}	DiM	0.1880	0.3741	1.4453	0.1712	0.6491	0.1480
H_{02}		1.7592	0.2204	0.4907	0.4739	0.6805	0.8564
H_{03}		1.0492	0.7910	0.6401	0.5173	0.5121	0.4063
H_0 by FCT		0.6871	0.2251	0.7674	0.1456	0.4888	0.1790
H_{01}	rs5	0.0608	0.0602	0.0844	0.0684	0.0752	0.0742
H_{02}		0.1418	0.1056	0.1388	0.1386	0.1210	0.1282
H_{03}		0.4283	0.4059	0.3675	0.3885	0.3509	0.4035
H_0 by FCT		0.0281	0.0212	0.0308	0.0283	0.0256	0.0291
H_{01}	rs20	0.0500	0.0530	0.2120	0.1016	0.1780	0.1588
H_{02}		0.1902	0.0868	0.2661	0.2695	0.1668	0.2200
H_{03}		0.5715	0.4875	0.5373	0.4827	0.4343	0.5131
H_0 by FCT		0.0369	0.0183	0.1298	0.0651	0.0700	0.0951

Table 6: Twice the median of p -values across repetitions. **Bold** denotes value below 0.05.

Results from the module sets that maximize expected number of active focal units Table 7 shows the test results for the beneficial spillover hypothesis (14) conducted on the module sets that maximize the expected number of active focal units among the 2,000 ones for all outcomes. Additionally, Table 8 presents the results for the crime displacement hypothesis (15) for all outcomes, conducted on the same module sets. We observe that similar conclusions to those in the main text for the crime index apply to other outcomes as well.

Hypothesis	test stat	homicides	assault	robbery	car theft	moto theft	crime index
H_{01}	DiM	0.1166	0.0990	0.5243	0.0358	0.0926	0.0108
H_{02}		0.8854	0.0620	0.1690	0.1798	0.6947	0.5379
H_{03}		0.7137	0.3837	0.1948	0.0746	0.2356	0.2002
H_0 by FCT		0.5164	0.0597	0.2295	0.0182	0.2116	0.0356
H_{01}	rs5	0.0102	0.0092	0.0130	0.0114	0.0106	0.0080
H_{02}		0.0418	0.0294	0.0558	0.0398	0.0448	0.0554
H_{03}		0.3059	0.2294	0.1938	0.2284	0.2144	0.1816
H_0 by FCT		0.0065	0.0036	0.0069	0.0054	0.0053	0.0044
H_{01}	rs20	0.0072	0.0054	0.0270	0.0112	0.0224	0.0108
H_{02}		0.0556	0.0226	0.1702	0.0834	0.0766	0.1640
H_{03}		0.4417	0.1516	0.2507	0.1672	0.2016	0.2797
H_0 by FCT		0.0083	0.0013	0.0353	0.0075	0.0141	0.0186

Table 7: Test p -values for the beneficial spillover hypothesis (14) using the module sets that maximize the expected number of active focal units. **Bold** denotes value below 0.05.

Hypothesis	test stat	homicides	assault	robbery	car theft	moto theft	crime index
H_{01}	DiM	0.8834	0.9010	0.4757	0.9642	0.9074	0.9892
H_{02}		0.1146	0.9380	0.8310	0.8202	0.3053	0.4621
H_{03}		0.2863	0.6163	0.8052	0.9254	0.7644	0.7998
H_0 by FCT		0.3133	0.9714	0.8913	0.9960	0.7957	0.9186
H_{01}	rs5	0.9898	0.9908	0.9870	0.9886	0.9894	0.9920
H_{02}		0.9582	0.9706	0.9442	0.9602	0.9552	0.9446
H_{03}		0.6941	0.7706	0.8062	0.7716	0.7856	0.8184
H_0 by FCT		0.9911	0.9964	0.9969	0.9960	0.9965	0.9974
H_{01}	rs20	0.9928	0.9946	0.9730	0.9888	0.9776	0.9892
H_{02}		0.9444	0.9774	0.8298	0.9166	0.9234	0.8360
H_{03}		0.5583	0.8484	0.7493	0.8328	0.7984	0.7203
H_0 by FCT		0.9720	0.9990	0.9854	0.9970	0.9954	0.9842

Table 8: Test p -values for the crime displacement hypothesis (15) using the module sets that maximize the expected number of active focal units. **Bold** denotes value below 0.05.

F.4 Monotone null hypothesis with six exposure levels

Instead of grouping exposures beyond 3 and test the monotone hypothesis in (14), here we group exposures at a higher threshold 5, so that $\mathcal{W} = \{0, 1, 2, 3, 4, [\geq 5]\}$, and test the following monotone hypothesis:

$$H_0 = \bigcap_{k \in [5]} H_{0k}, \text{ where} \tag{24}$$

$$H_{01} : y_i(0, 0) \geq y_i(0, 1), \quad H_{02} : y_i(0, 1) \geq y_i(0, 2), \quad H_{03} : y_i(0, 2) \geq y_i(0, 3),$$

$$H_{04} : y_i(0, 3) \geq y_i(0, 4), \quad H_{05} : y_i(0, 4) \geq y_i(0, [\geq 5]), \quad \forall i.$$

We are still testing the beneficial (harmless) hypothesis that when more nearby units are treated the crime in the current street is lower. We again adjust $\Delta Y_i = Y_i^{\text{post}} - Y_i^{\text{pre}}$ for the five types of crime and the crime index, and consider the difference-in-means and the Stephenson rank sum test statistics with $s = 5, 20$, with p -values combined by Fisher’s rule.

Figure 18 shows the histograms of the numbers of eligible and active focal units across the 2,000 random constructions of module sets, and Table 9 shows twice the median of p -values resulting from applying Algorithm 2 on these 2,000 module sets. Two of the 2,000 realizations are presented in Figure 19. We observe similar patterns as in testing four exposure

levels in Section 7, that focal units used to test hypotheses involving lower exposure contrast tend to spread at the outskirts, while focal units for hypotheses involving higher exposure contrast tend to be in the center of the city. Table 10 reports the result when we apply the test on the module sets with the largest expected number of active focal units. The results from Table 10 still reject the beneficial null (24), and the rejection signals again mainly come from individual contrast hypotheses involving lower exposure levels. In this case, however, twice the median of p -values across repetitions become less powerful.

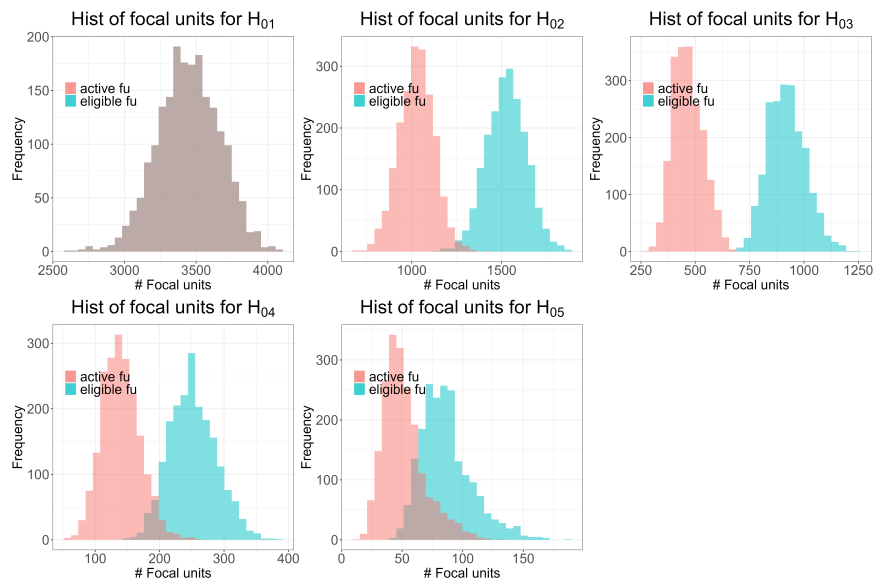


Figure 18: Histograms of number of focal units across the 2,000 repetitions, for the null (24).

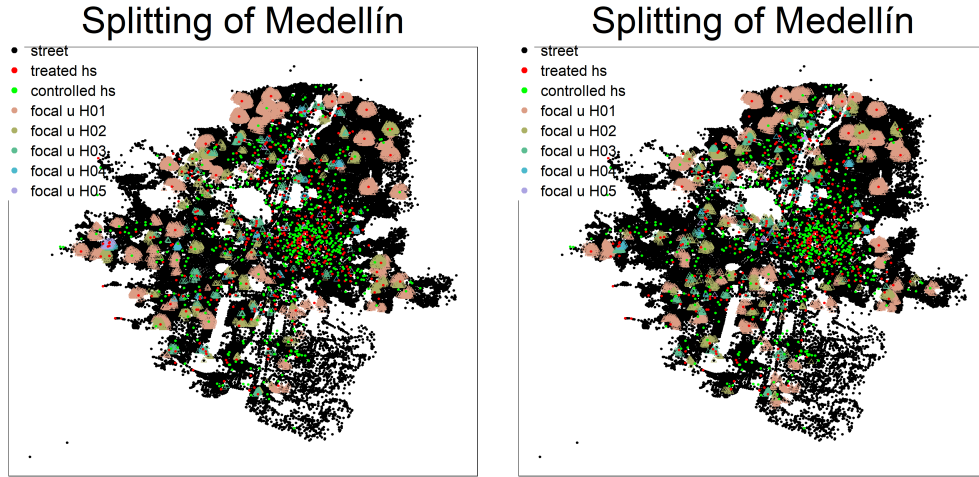


Figure 19: Two realizations of focal units for testing under $\mathcal{W} = \{0, 1, 2, 3, 4, [\geq 5]\}$.

Hypothesis	test stat	homicides	assault	robbery	car theft	moto theft	crime index
H_{01}	DiM	0.2559	0.3885	1.4425	0.2190	0.5819	0.1750
H_{02}		1.7962	0.1744	0.4449	0.4027	0.7315	0.8566
H_{03}		1.2304	0.7407	0.3919	0.3747	0.8376	0.5235
H_{04}		1.1424	1.1740	0.4782	0.9213	0.5259	0.5455
H_{05}		1.1852	1.1622	1.3965	1.2170	1.2034	1.3709
H_0 by FCT		1.0546	0.3616	0.5379	0.2351	0.6006	0.3128
H_{01}	rs5	0.0860	0.0856	0.1118	0.0928	0.0996	0.0988
H_{02}		0.1438	0.1046	0.1392	0.1372	0.1252	0.1308
H_{03}		0.3763	0.3609	0.2875	0.3297	0.3349	0.3693
H_{04}		1.0216	1.2274	1.0192	1.0564	0.9492	0.9618
H_{05}		0.8530	0.8204	1.0296	0.8250	0.8656	0.9980
H_0 by FCT		0.0580	0.0523	0.0590	0.0526	0.0517	0.0610
H_{01}	rs20	0.0748	0.0776	0.2272	0.1224	0.1902	0.1784
H_{02}		0.1936	0.0872	0.2613	0.2426	0.1754	0.2509
H_{03}		0.4795	0.4223	0.3131	0.3913	0.4269	0.4421
H_{04}		0.9496	1.4525	1.1354	1.1928	0.9202	0.9762
H_{05}		0.8760	0.8258	1.1994	0.8004	0.8858	1.1252
H_0 by FCT		0.0764	0.0618	0.1845	0.1069	0.1261	0.1660

Table 9: Twice the median of p -values across repetitions for the null (24).

Hypothesis	test stat	homicides	assault	robbery	car theft	moto theft	crime index
H_{01}	DiM	0.1566	0.2352	0.7564	0.0980	0.0614	0.0346
H_{02}		0.7097	0.0466	0.0816	0.0548	0.6769	0.2649
H_{03}		0.9242	0.4089	0.3915	0.2613	0.1602	0.3707
H_{04}		0.8126	0.6397	0.1552	0.1718	0.5839	0.4265
H_{05}		0.3877	0.4073	0.8802	0.3885	0.1872	0.3825
H_0 by FCT		0.7384	0.1967	0.3252	0.0463	0.1533	0.1322
H_{01}	rs5	0.0732	0.0754	0.0936	0.0804	0.0872	0.0804
H_{02}		0.0016	0.0012	0.0008	0.0014	0.0016	0.0008
H_{03}		0.1846	0.1510	0.1212	0.1530	0.1152	0.1246
H_{04}		0.4359	0.5433	0.3847	0.3973	0.3999	0.3909
H_{05}		0.3077	0.2308	0.4267	0.3349	0.2314	0.2705
H_0 by FCT		0.0045	0.0031	0.0028	0.0038	0.0028	0.0018
H_{01}	rs20	0.0566	0.0712	0.1790	0.1050	0.1830	0.1246
H_{02}		0.0020	0.0006	0.0030	0.0006	0.0070	0.0022
H_{03}		0.2478	0.1332	0.1574	0.1732	0.0866	0.1398
H_{04}		0.4359	0.7129	0.3567	0.4397	0.4213	0.3321
H_{05}		0.3163	0.0646	0.7343	0.4503	0.1484	0.2671
H_0 by FCT		0.0055	0.0008	0.0182	0.0036	0.0083	0.0050

Table 10: Test p -values for the null (24) using the module sets that maximize the expected number of active focal units. **Bold** denotes value below 0.05.